Supporting Information

Design, synthesis and biological evaluation of oxalamide derivatives as potent neuraminidase inhibitors

Xing Yong Zhang, Li Ping Cheng*, Zhi Jian Zhong, Wan Pang*, Xue Song

Contents

1. Database preparation

In the primary docking-based virtual screening, the compounds were obtained from the ZINC 12 database (http://www.zinc12.docking.org/). These small compounds were downloaded in "sdf format" and then converted to "sln format" by the software SYBYL-X 2.1 (Tripos, Inc., USA).

2. Molecular docking and MD simulations

Molecular docking technique is an important method to study the interaction mechanism between small molecules and proteins macromolecules.[1,2] The Surflex-Dock module was used for molecular docking in SYBYL-X 2.1 (Tripos, Inc., USA). Docking score was used to examine the affinity between the ligand and the receptor. The higher the total-score value is, the better the docking result is. The crystal structure of the neuraminidase protein complex (PDB ID: 2HU0)[3] was taken from the RSCB protein database (http://www.rcsb.org/pdb/). The X-ray coordinates of neuraminidase (PDB ID: 2HU0) had been listed in the Table S2. The protein crystal was used as a template to the primary docking-based virtual screening. Before the docking calculations were performed, a series of necessary preparations of protein need to be treated such as removing water molecules and non-ligand structures in protein crystals, protonating amino acid residues such as Asp and Glu in active site. The AMBER-FF99[4] atomic type and Gasteiger-Huckel charge were added to the ligand. The complex protein was optimized by AMBER7 FF99 force field and molecular docking was performed according to the generated protomol file to obtain the corresponding docking score. All of the above protein preparation processes are achieved through the SYBYL-X 2.1 biopolymer module. The docked pose selection should satisfy the following criteria: 1) a correct pose is usually regarded as matching the pose in a cocrystallized protein or enzyme; 2) The higher the total-score value is, the better the docked pose is. 3) The docked pose could interact well with some key amino acids at the active site of NA, such as Arg118, Arg292, Arg371, which are essential for the NA inhibitory activity.

In this work, the 4-chloro and 3-fluorine substituted phenyl group had been given priority from the beginning. However, as shown in Fig. S1, the molecular docking results shows that 4-chloro substituted phenyl in **Z11** could not well occupy the 430-cavity but stretches out of the 430-cavity. The 3-fluorine substituted phenyl in **Z12** and 3-methoxy substituted phenyl in **Z13** could not fully extend into the 430-cavity. Table S1 shows that the total scores of these three compounds are all far lower than

other synthesized target compounds and lead compound **5**. Therefore, the activities against NA of the three compounds **Z11**-**Z13** are theoretically poor, they were excluded from the synthesized target compounds and had not been performed further study. The reason why the 3-chloro, 2-methoxy instead of 4-fluorine substituted phenyl of the lead compound **5** should also be attributed to the molecular docking study. After the most potent **Z2** was synthesized, the introduction of 4-fluorine substituted phenyl had been tried and the corresponding compound **Z14** had been designed. However, as shown in Fig. S1, the 4-fluorine substituted phenyl of **Z14** also stretches out of the 430-cavity, the docking score is as low as 7.05, indicating its poor activity. Therefore, **Z14** was also excluded from the synthesized target compounds and had not been performed further study.

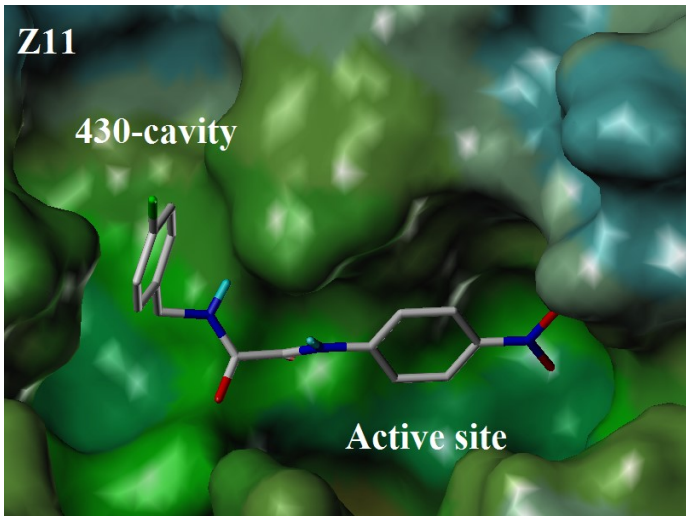

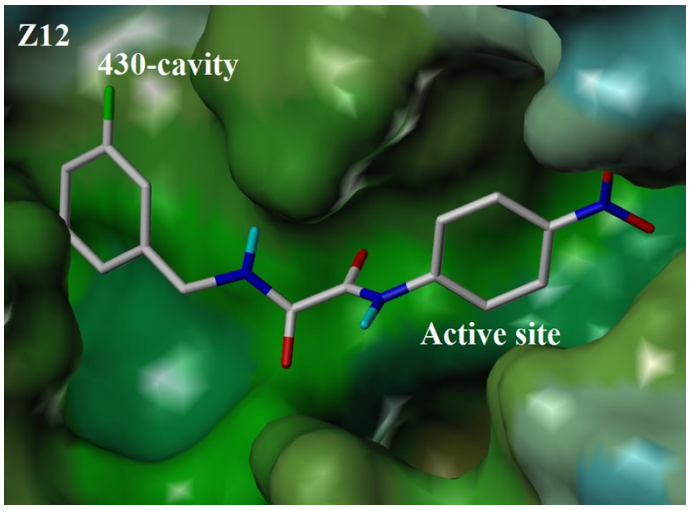

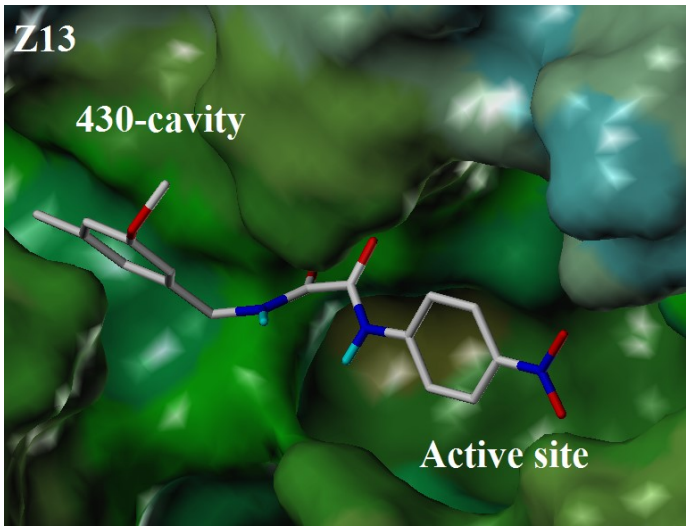

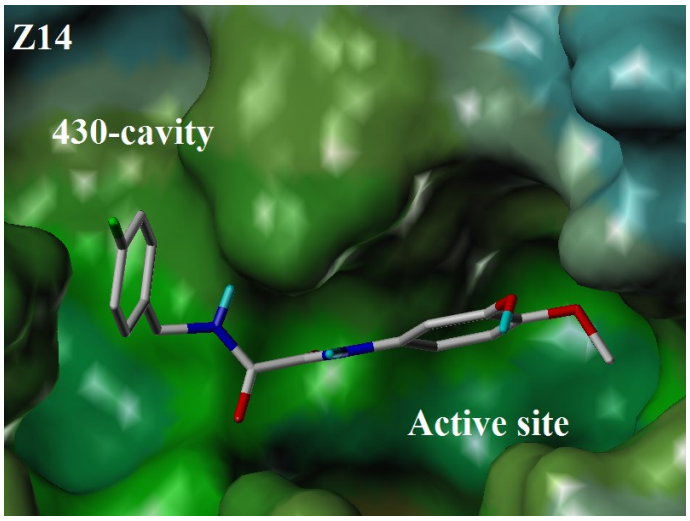

Fig. S1 Molecular docking results of designed compounds **Z11-Z14** with NA (show only polar hydrogens)

Table S1. The docking scores of some designed compounds with NA

Compound	Structure	Total score
5	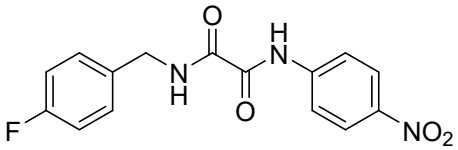	9.9735
Z2	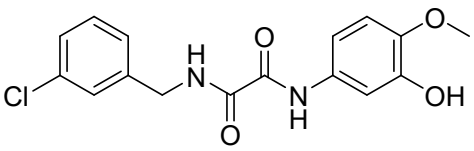	11.4908

Z5	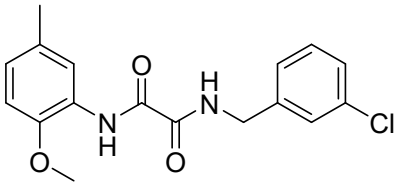	10.5130
Z10	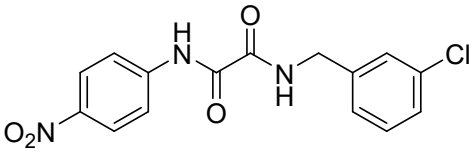	10.1822
Z11	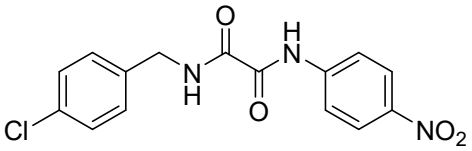	5.6073
Z12	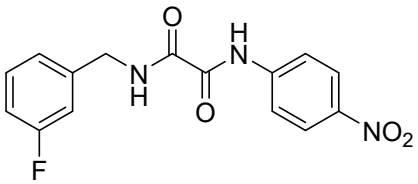	6.0449
Z13	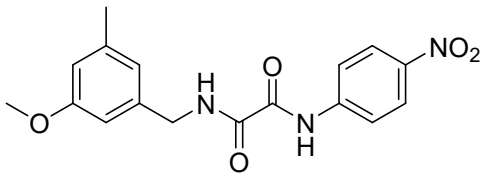	5.3957
Z14	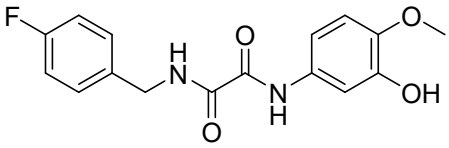	7.0530

In order to verify the reliability of molecular docking, the molecular dynamics simulations (MD) of the compound molecules and neuraminidase protein were performed under the Linux system with Amber 12.0 software packages.[5] The ff99SB[6] force field and the AMBER force field (gaff)[7] were added to the protein and ligand compounds respectively. The counter-ions, Na^+ or Cl^-, were added to neutralize the unbalanced charges in the complexes.[8] The particle mesh Ewald (PME) algorithm[9] of the electrostatic term was defined as a dielectric constant of 1.0 and a cutoff 10.0 Å. In order to reduce the computational demand, each system was added 10 Å out of the solute with an octahedral TIP3P water box. In the initial optimization step is performed by the Sander package in amber, the atomic positions of all solutes are bound by 100 $kal \cdot mol^{-1} \cdot Å^{-2}$. The whole system is minimized without binding force, which is reduced by 1000 steps of steepest descent method and then by 4000 steps of

conjugated gradient method. Then, the system is gradually heated from 0 to 300 K over a period of 20 ps in the NVT ensemble, and balanced in NPT system at 300 K over 100 ps. Finally, a dynamic simulation process of 20 ns was carried out under the condition of 300 K with 1.0 atm and the NMR condition is closed. During the whole MD operation, the coordinate displacement is recorded per 2 ps. VMD is used for visualization and analysis. The selected compounds were subjected to RMSD and cluster analysis using the Xmgrace program. The binding free energy of the ligand-neuraminidase protein complex was calculated by Molecular Mechanics/Generalized Born Surface Area (MM/GBSA) and Molecular Mechanics/Poisson Boltzman Surface Area (MM/PBSA).[10-12] The stable conformation generated by the last 2 ns was used to calculate the binding free energy (ΔG_{bind}), which was calculated as follows:

$$\Delta G_{bind} = \Delta H - T\Delta S \approx \Delta G_{gas} + \Delta G_{sol} - T\Delta S;$$
$$\Delta G_{gas} = \Delta E_{ele} + \Delta E_{vdw}; \Delta G_{sol} = \Delta G_{PB\,/\,GB} + \Delta G_{SA}$$

ΔG_{gas} represents the gas phase interaction energy between protein and ligand, including electrostatic energy (ΔE_{ele}) and van der Waals energy (ΔE_{vdw}). ΔG_{sol} is the sum of $\Delta G_{\text{PB/GB}}$ electrostatic solvation energy (polarity contribution) and non-electrostatic solvation component (non-polar contribution) ΔG_{SA}. In this work, the calculation of entropy change is not considered, because its calculation process is very time-consuming and the calculation accuracy is low. Table S3 shows the binding free energies obtained by the two calculated methods for the three compounds in the **Data set 4** and the reference OSC. The corresponding RMSD values were shown in Fig. S2.

Table S2. Crystallographic data and refinement statistics

PDB ID	2HU0
Space group	C 2 2 21
Cell constants a, b, c, α, β, γ	198.08 Å 200.58 Å 210.42 Å 90.00° 90.00° 90.00°
Resolution (Å)	142.86 – 2.95 19.70 – 2.86
% Data completeness (in resolution range)	79.1 (142.86 – 2.95) 77.7 (19.70 – 2.86)
R_{sym}	Not available
R_{merge}	Not available
R, R_{free}	0.218, 0.295 0.255, 0.258
Anisotropy	0.061

Total number of atoms	23716
Wilson B-factor (Å^2)	32.1
Refinement program	REFMAC 5.2.0019
Bulk solvent κ_{sol} (e/Å^3), *Bsol* (Å^2)	0.29, -18.6
Average B, all atoms (Å^2)	24.0

Table S3. Predicted binding free energies of **Data set 4** and the reference OSC by MM/PBSA and MM/GBSA methods.

Compound	VDW	EEL	ΔG_{gas}	ΔG_{GB}	ΔG_{SA}	ΔG_{solv}(GB)	ΔG_{bind}(GB)	ΔG_{PB}	ΔG_{SA}	ΔG_{solv}(PB)	ΔG_{bind}(PB)
OSC	-30.36	-24.18	-54.54	45.44	-4.30	41.14	-13.40	48.15	-3.69	44.46	-10.08
ZINC05250774	-30.22	-13.72	-43.94	30.46	-3.69	26.77	-17.18	32.32	-3.22	29.10	-14.84
ZINC57589121	-23.77	-13.25	-37.02	24.79	-3.23	21.56	-15.46	25.56	-2.86	22.70	-14.32
ZINC08458181	-19.60	-8.80	-28.40	18.22	-2.56	15.66	-12.73	17.47	-2.33	15.15	-13.25

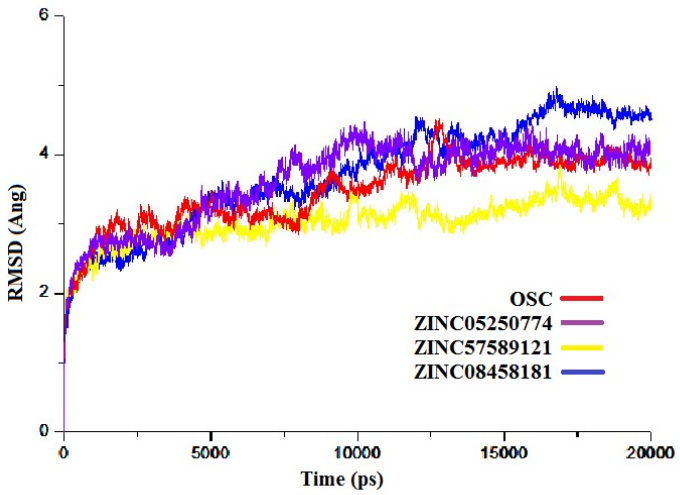

Fig. S2 The RMSD values of the compounds of **Data set 4** and reference OSC with NA versus simulation time.

3. Chemistry materials and methods

All the chemical regents were commercially available regents without further purification. To monitor the reaction by thin layer chromatography (TLC) with precoated silica gel 60 F254. ^{1}H NMR and ^{13}C NMR spectra were recorded on a Bruker AVANCE III at 400 MHz, 100 MHz in DMSO-d_6 using TMS (δ= 2.50 ppm) as internal standard. Chemical shifts are reported in δ (parts per million (ppm)) with TMS and coupling constants (*J*) in Hz. HRMS were recorded on a solariX 70 FTMS spectrometer (Bruker) using methanol and acetonitrile as the solvent. Data were

acquired in the positive ion mode at resolving power of 100,000. Melting points were measured using a WRS-2A digital melting point apparatus (Shanghai Shenguang Instrument Co., Ltd., Shanghai China). Analytic HPLC was performed on Agilent technologies 1260 series with water contains 0.1% CH_3COOH (Solvent B, 40%)/CH_3CN (Solvent A, 60%) as eluent and the targeted products were detected by DAD in the detection rang of 254-320 nm. Product purities were confirmed to be >95% by this method.

3.1 General procedure for synthesis of 7

A mixture of the substituted aniline (20 mmol) and triethylamine (4.17 mL, 30 mmol) in ethyl acetate (80.00 mL) was stirred at 0℃. Oxalyl chloride monoethyl ester (3.36 mL, 30 mmol) was added dropwise to a cooled stirred mixture for 0.5 h. This solution was stirred at room temperature for 6 h. After the reaction was completed, the reaction mixture was quenched with distilled water and then was extracted three times with 100 mL of ethyl acetate. After separation of the phases, the organic layer was washed twice with 1 M hydrochloric acid and twice with saturated sodium bicarbonate solution, followed by drying with anhydrous sodium sulfate and evaporation of the solvent in vacuo. The crude product was purified by column chromatography to obtain the compound **7**.

ethyl 2-((3-chlorobenzyl)amino)-2-oxoacetate(7a)

White solid, yield 88.7%, ^{1}H NMR (400 MHz, DMSO-d_6) δ 8.48 (t, J = 6.1 Hz, 1H), 7.37 – 7.28 (m, 3H), 7.20-7.17 (m, 1H), 4.41 (dt, J = 6.2, 1.0 Hz, 2H), 4.30 (q, J = 7.1 Hz, 2H), 1.40 (t, J = 7.1 Hz, 3H). ^{13}C NMR (100 MHz, DMSO-d_6) δ 161.88, 161.31, 138.62, 133.61, 129.55, 127.80, 127.76, 126.39, 62.98, 43.45, 13.99.

ethyl 2-((2-methoxy-5-methylphenyl)amino)-2-oxoacetate(7b)

Yellow solid, yield 87.3%, ^{1}H NMR (400 MHz, DMSO-d_6) δ 10.54 (s, 1H), 8.24 (d, J = 1.9 Hz, 1H), 7.15 – 6.99 (m, 2H), 4.34 (q, J = 7.1 Hz, 2H), 3.88 (s, 3H), 2.30 (s, 3H), 1.40 (t, J = 7.0 Hz, 3H). ^{13}C NMR (100 MHz, DMSO-d_6) δ 161.01, 156.66, 146.66, 133.41, 127.30, 124.18, 120.89, 111.82, 62.98, 56.01, 20.97, 14.39.

ethyl 2-((4-nitrophenyl)amino)-2-oxoacetate(7c)

White solid, yield 89.1%,^{1}H NMR (400 MHz, DMSO-d_6) δ 8.30 – 8.19 (m, 4H), 4.35 (q, J = 7.1 Hz, 2H), 1.38 (t, J = 7.1 Hz, 3H). ^{13}C NMR (100 MHz, DMSO-d_6) δ 161.35, 156.44, 143.41, 141.60, 125.52, 118.04, 62.99, 13.95.

3.2 General procedure for synthesis of 8

Potassium hydroxide (1.68 g, 30 mmol) dissolved in 5 mL of distilled water was

added to a solution of compound **7** (10 mmol) in 150 mL ethanol at 0 ℃. The reaction mixture was allowed to warm to room temperature and stirred for additional 4 h. After the reaction was completed, 100 mL of distilled water was added to the reaction solution and the solution was acidified with concentrated hydrochloric acid to pH 1. After removing the solvent in vacuo, compound **8** was recrystallized from water.

2-((3-chlorobenzyl)amino)-2-oxoacetic acid(8a)

White solid, yield 82.6%, ^{1}H NMR (400 MHz, DMSO-d_6) δ 9.13 (s, 1H), 8.55 (t, J = 6.1 Hz, 1H), 7.36 – 7.25 (m, 3H), 7.20-7.17 (m, 1H), 4.49(dt, J = 6.0, 0.9 Hz, 2H). ^{13}C NMR (100 MHz, DMSO-d_6) δ 162.85, 162.80, 138.59, 133.77, 129.47, 127.90, 126.74, 126.31, 43.64.

2-((2-methoxy-5-methylphenyl)amino)-2-oxoacetic acid(8b)

Yellow solid, yield 83.5%, ^{1}H NMR (400 MHz, DMSO-d_6) δ 10.12 (s, 1H), 9.39 (s, 1H), 8.17 (d, J = 1.8 Hz, 1H), 7.10 – 6.99 (m, 2H), 3.91 (s, 3H), 2.36 (s, 3H). ^{13}C NMR (100 MHz, DMSO-d_6) δ 162.60, 161.18, 146.91, 133.33, 127.69, 124.09, 120.87, 111.65, 56.01, 20.94.

2-((4-nitrophenyl)amino)-2-oxoacetic acid(8c)

White solid, yield 81.7%,^{1}H NMR (400 MHz, DMSO-d_6) δ 9.50 (s, 1H), 8.36 – 8.27 (m, 2H), 8.22 – 8.15 (m, 2H). ^{13}C NMR (100 MHz, DMSO-d_6) δ 163.02, 160.85, 143.60, 142.33, 125.49, 118.14.

3.3 General procedure for synthesis of target compounds Z1-Z10

Compound **8** (5 mmol) and substituted aniline (7.5 mmol) were dissolved in DMF (50 mL), and then HOBt (1.35g, 10 mmol) and EDCl (3.35g, 17.5 mmol) were added into the solution. The reaction mixture was stirred at 25 ℃ for 6 h under nitrogen flow condition. After completion of the reaction, the precipitate was filtered, washed by distilled water. The crude product was recrystallized by 95% aqueous ethanol to give the appropriate target compounds **Z1-Z10**.

N^1-(3-chlorobenzyl)-N^2-(3,4,5-trimethoxyphenyl)oxalamide (Z1). White solid, yield 81%, m.p.215.5-215.7℃, purity 98.66%; ^{1}H NMR (400 MHz, DMSO-d_6) δ 10.55 (s, 1H), 9.59 (t, J = 6.4 Hz, 1H), 7.42 – 7.29 (m, 6H), 4.42 (d, J = 6.4 Hz, 2H), 3.77 (s, 6H), 3.66 (s, 3H). ^{13}C NMR (100 MHz, DMSO-d_6) δ 160.75, 158.67, 153.11, 141.66, 134.82, 134.11, 133.46, 130.71, 127.71, 127.43, 126.54, 98.79, 60.58, 56.23, 42.58. HRMS (ESI) calcd for $C_{18}H_{19}ClN_2O_5$[M+Na]$^+$: 401.0875; Found: 401.0871.

N^1-(3-chlorobenzyl)-N^2-(3-hydroxy-4-methoxyphenyl)oxalamide (Z2). Brown solid, yield 85%, m.p172.4-173.4℃, purity 98.68%; ^{1}H NMR (400 MHz, DMSO-d_6) δ

10.39 (s, 1H), 9.52 (t, *J* = 6.4 Hz, 1H), 9.07 (s, 1H), 7.41 – 7.36 (m, 3H), 7.34 (dd, *J* = 6.5, 1.7 Hz, 1H), 7.29 (d, *J* = 7.3 Hz, 1H), 7.20 (dd, *J* = 8.7, 2.5 Hz, 1H), 6.89 (d, *J* = 8.8 Hz, 1H), 4.40 (d, *J* = 6.4 Hz, 2H), 3.76 (s, 3H). ^{13}C NMR (100 MHz, DMSO-d_6) δ 161.00, 158.37, 146.76, 145.23, 141.75, 133.43, 131.54, 130.71, 127.79, 127.42, 126.62, 112.73, 111.84, 109.20, 56.34, 42.58. HRMS (ESI) calcd for $C_{16}H_{15}ClN_2O_4$[M+Na]$^+$: 357.0613; Found: 357.0607.

N*^{1}*-(3-chlorobenzyl)-N*^{2}*-(3-fluorophenethyl)oxalamide (Z3). White solid, yield 79%, m.p.142.5-143.5℃, purity 98.39%; ^{1}H NMR (400 MHz, DMSO-d_6) δ 9.35 (t, *J* = 6.4 Hz, 1H), 8.85 (t, *J* = 5.9 Hz, 1H), 7.40 – 7.30 (m, 4H), 7.22 (d, *J* = 7.3 Hz, 1H), 7.09 – 7.00 (m, 3H), 4.33 (d, *J* = 6.5 Hz, 2H), 3.43 (dd, *J* = 13.6, 6.9 Hz, 2H), 2.84 (t, *J* = 7.2 Hz, 2H). ^{13}C NMR (100 MHz, DMSO-d_6) δ 163.87, 161.46, 160.68, 160.27, 142.61, 141.79, 133.41, 130.67, 130.54, 127.63, 127.36, 126.47, 125.28, 115.89, 113.32, 42.33, 34.62. HRMS (ESI) calcd for $C_{17}H_{16}ClF_2O_2$[M+H]$^+$: 335.0957; Found: 335.0961.

N*^{1}*-(2-(benzo[d][1,3]dioxol-5-yl)ethyl)-N*^{2}*-(3-chlorobenzyl)oxalamide (Z4). White solid, yield 89%, m.p151.9-153.1℃, purity 99.43%; ^{1}H NMR (400 MHz, DMSO-d_6) δ 9.34 (t, *J* = 6.4 Hz, 1H), 8.76 (t, *J* = 5.9 Hz, 1H), 7.37 – 7.30 (m, 3H), 7.23 (d, *J* = 7.3 Hz, 1H), 6.81 (dd, *J* = 7.6, 4.6 Hz, 2H), 6.66 (dd, *J* = 7.9, 1.5 Hz, 1H), 5.98 (s, 2H), 4.33 (d, *J* = 6.5 Hz, 2H), 3.40 – 3.35 (m, 2H), 2.73 (t, *J* = 7.3 Hz, 2H). ^{13}C NMR (100 MHz, DMSO-d_6) δ 160.75, 160.22, 147.69, 146.04, 141.80, 133.42, 133.36, 130.68, 127.66, 127.37, 126.50, 121.98, 109.44, 108.57, 101.15, 42.35, 41.00, 34.72. HRMS (ESI) calcd for $C_{18}H_{17}Cl_2O_4$[M+NH$_4$]$^+$: 378.1215; Found: 378.1221.

N*^{1}*-(3-chlorobenzyl)-N*^{2}*-(2-methoxy-5-methylphenyl)oxalamide (Z5). Yellow solid, yield 78%, m.p.168.0-169.2℃, purity 99.53%; ^{1}H NMR (400 MHz, DMSO-d_6) δ 9.75 (s, 1H), 9.68 (t, *J* = 6.4 Hz, 1H), 8.02 (d, *J* = 1.5 Hz, 1H), 7.42 – 7.27 (m, 4H), 7.03 – 6.95 (m, 2H), 4.41 (d, *J* = 6.4 Hz, 2H), 3.87 (s, 2H), 2.28 (s, 3H). ^{13}C NMR (100 MHz, DMSO-d_6) δ 160.53, 157.52, 147.30, 141.46, 133.46, 130.73, 129.95, 127.81, 127.50, 126.66, 125.91, 120.50, 111.53, 56.53, 42.80, 21.03. HRMS (ESI) calcd for $C_{17}H_{17}ClN_2O_3$[M+Na]$^+$: 355.0820; Found: 355.0824.

N*^{1}*-(3-hydroxy-4-methoxyphenyl)-N*^{2}*-(2-methoxy-5-methylphenyl)oxalamide (Z6). Brown solid, yield 86%, m.p.175.8-176.6℃, purity 99.08%; ^{1}H NMR (400 MHz, DMSO-d_6) δ 10.67 (s, 1H), 9.86 (s, 1H), 9.12 (s, 1H), 8.05 (s, 1H), 7.41 (s, 1H), 7.26 (d, *J* = 8.7 Hz, 1H), 7.02 (dd, *J* = 17.7, 8.3 Hz, 2H), 6.92 (d, *J* = 8.7 Hz, 1H), 3.89 (s, 3H), 3.77 (s, 3H), 2.30 (s, 3H). ^{13}C NMR (100 MHz, DMSO-d_6) δ 158.17, 157.89, 147.40, 146.79, 145.48, 131.29, 129.96, 128.06, 125.98, 120.56, 112.65, 112.09,

111.59, 109.40, 56.32, 21.08. HRMS (ESI) calcd for $C_{17}H_{18}N_2O_5[M+H]^+$: 331.1288; Found: 331.1291.

N^1-(3-fluorophenethyl)-N^2-(2-methoxy-5-methylphenyl)oxalamide (Z7). White solid, yield 83%, m.p.104.5-105.4℃, purity 99.67%; ^{1}H NMR (400 MHz, DMSO-d_6) δ 9.72 (s, 1H), 9.13 (t, *J* = 5.5 Hz, 1H), 8.01 (s, 1H), 7.35 (dd, *J* = 14.7, 7.5 Hz, 1H), 7.11 – 6.93 (m, 5H), 3.87 (s, 3H), 3.47 (dd, *J* = 13.6, 6.8 Hz, 2H), 2.88 (t, *J* = 7.2 Hz, 2H), 2.27 (s, 3H). ^{13}C NMR (100 MHz, DMSO-d_6) δ 161.48, 160.17, 157.57, 147.20, 142.44, 130.70, 129.96, 125.90, 125.85, 125.31, 120.33, 115.71, 113.58, 111.52, 56.53, 40.85, 34.51, 21.03. HRMS (ESI) calcd for $C_{18}H_{19}FN_2O_3[M+Na]^+$: 353.1272; Found: 353.1274.

N^1-(2-(benzo[d][1,3]dioxol-5-yl)ethyl)-N^2-(2-methoxy-5-methylphenyl)oxalamide (Z8). White solid, yield 88%, m.p.141.5-142.4℃, purity 97.75%; ^{1}H NMR (400 MHz, DMSO-d_6) δ 9.73 (s, 1H), 9.07 (s, 1H), 7.99 (d, *J* = 19.0 Hz, 1H), 7.05 – 6.95 (m, 2H), 6.83 (d, *J* = 9.1 Hz, 2H), 6.68 (d, *J* = 7.9 Hz, 1H), 5.98 (s, 2H), 3.88 (d, *J* = 11.3 Hz, 3H), 3.42 (s, 2H), 2.76 (t, *J* = 7.0 Hz, 2H), 2.29 (d, *J* = 8.9 Hz, 3H). ^{13}C NMR (100 MHz, DMSO-d_6) δ 160.09, 157.58, 147.66, 147.17, 146.05, 133.23, 129.97, 125.89, 125.83, 122.05, 120.30, 111.48, 109.47, 108.63, 101.15, 56.49, 41.41, 34.58, 21.01. HRMS (ESI) calcd for $C_{19}H_{20}N_2O_5[M+H]^+$: 357.1145; Found: 357.1149.

N^1-(4-nitrophenyl)-N^2-(3,4,5-trimethoxyphenyl)oxalamide (Z9). White solid, yield 73%, m.p.193.5-194.3℃, purity 99.17%; ^{1}H NMR (400 MHz, DMSO-d_6) δ 11.44 (s, 1H), 10.85 (s, 1H), 8.31 (d, *J* = 9.1 Hz, 2H), 8.16 (d, *J* = 9.1 Hz, 2H), 7.38 (s, 2H), 3.79 (s, 6H), 3.67 (s, 3H). ^{13}C NMR (100 MHz, DMSO-d_6) δ 159.73, 158.19, 153.13, 144.28, 143.74, 134.90, 134.04, 125.27, 120.81, 98.76, 60.60, 56.19. HRMS (ESI) calcd for $C_{17}H_{17}N_3O_7[M+H]^+$: 376.1139; Found: 376.1144.

N^1-(3-chlorobenzyl)-N^2-(4-nitrophenyl)oxalamide (Z10). Yellow solid, yield 84%, m.p.185.9-186.3℃, purity 99.11%; ^{1}H NMR (400 MHz, DMSO-d_6) δ 11.26 (s, 1H), 9.70 (t, *J* = 6.3 Hz, 1H), 8.28 (d, *J* = 9.2 Hz, 2H), 8.13 (d, *J* = 9.2 Hz, 2H), 7.41 (s, 1H), 7.38 (d, *J* = 7.5 Hz, 1H), 7.34 (d, *J* = 6.6 Hz, 1H), 7.30 (d, *J* = 7.3 Hz, 1H), 4.43 (d, *J* = 6.4 Hz, 2H). ^{13}C NMR (100 MHz, DMSO-d_6) δ 160.20, 159.73, 144.28, 143.69, 141.51, 133.46, 130.71, 127.80, 127.47, 126.63, 125.18, 120.89, 42.67. HRMS (ESI) calcd for $C_{15}H_{12}ClN_3O_4[M+Na]^+$: 356.0409; Found: 356.0413.

4. ^{1}H NMR, ^{13}C NMR and HRMS spectra for the target compounds Z1-Z10

Z1

1

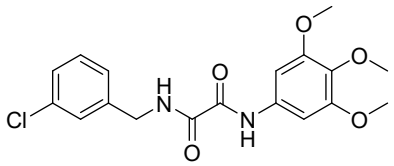
Cl
H
N
O
O
N
H
O
O
O

2

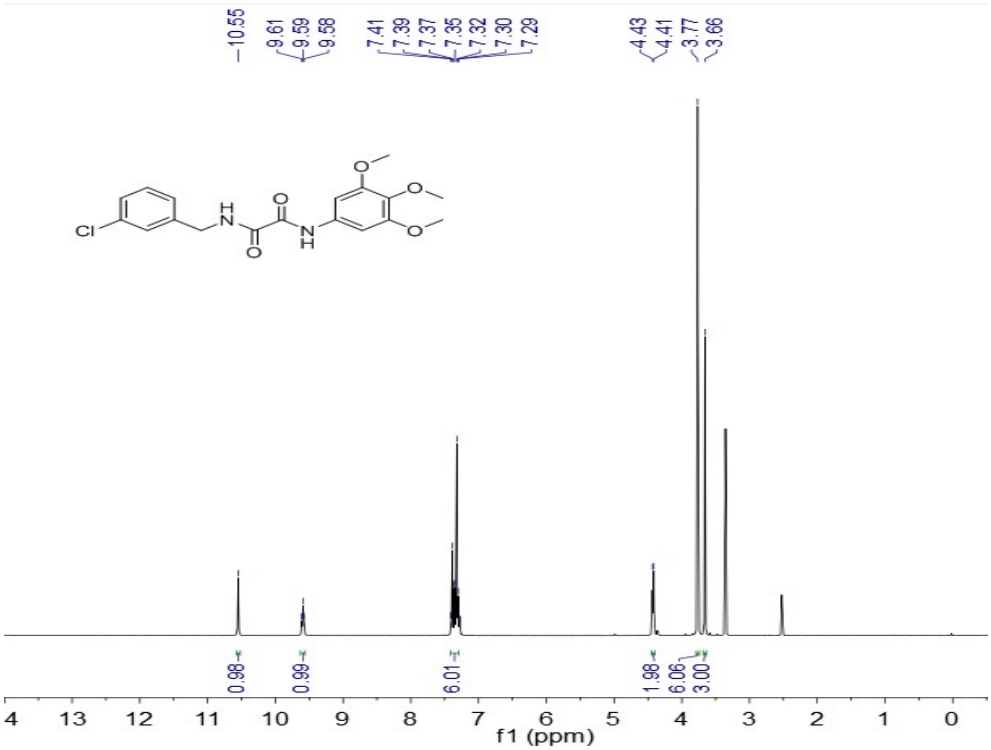
10.55
9.61
9.59
9.58
7.41
7.39
7.37
7.35
7.32
7.30
7.29
4.43
4.41
3.77
3.66
0.98
0.99
6.01
1.98
6.06
3.00
f1 (ppm)

3

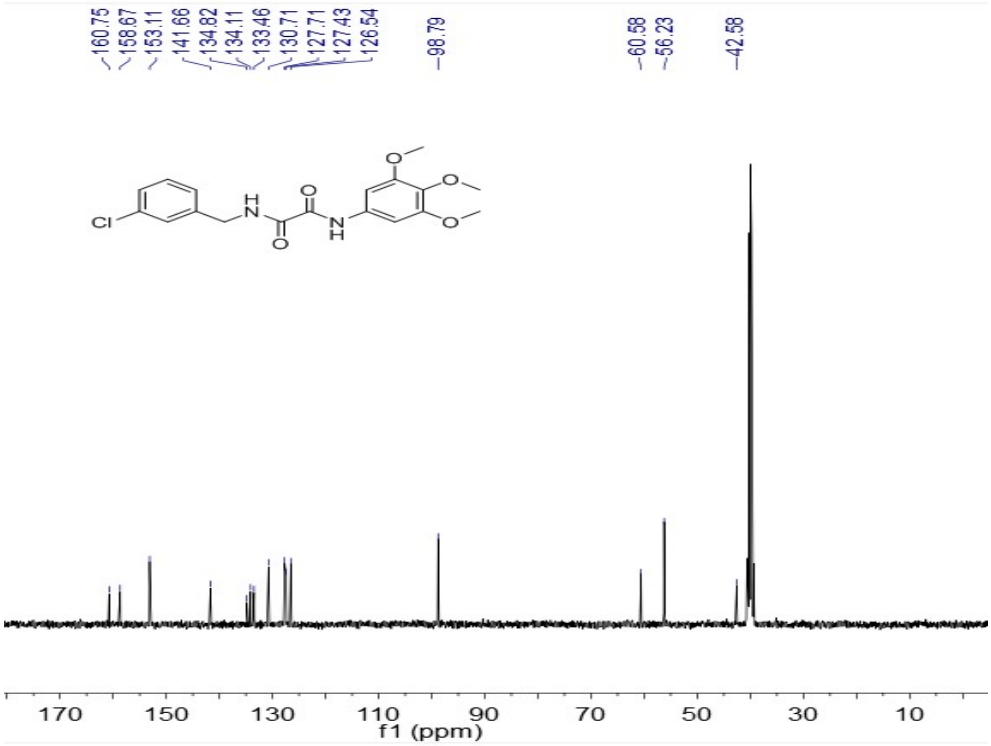
160.75
158.67
153.11
141.66
134.82
134.11
133.46
130.71
127.71
127.43
126.54
98.79
60.58
56.23
42.58
f1 (ppm)

System Verification of Internal Mass Accuracy ESI Mode

Analysis Info

Analysis Name	D:\Data\HYY\CLP_000378.d	Acquisition Date	6/2/2021 2:18:14 PM
Method	4_19_MassAccuNeg	Operator	
Sample Name	58	Instrument	solariX
Comment	Glu-Fib 250amol		

Acquisition Parameter

Polarity	Positive	n/a	n/a	No. of Laser Shots	200
n/a	n/a	No. of Cell Fills	1	Laser Power	20.0 lp
Broadband Low Mass	53.8 m/z	n/a	n/a	n/a	n/a
Broadband High Mass	1000.0 m/z	n/a	n/a	n/a	n/a
Acquisition Mode	Single MS	n/a	n/a		
Pulse Program	basic	n/a	n/a	Calibration Date	Fri Feb 21 02:36:54 2014
Source Accumulation	0.020 sec	n/a	n/a	Data Acquisition Size	1048576
Ion Accumulation Time	0.200 sec	n/a	n/a	Apodization	Sine-Bell Multiplication
Flight Time to Acq. Cell	0.001 sec				

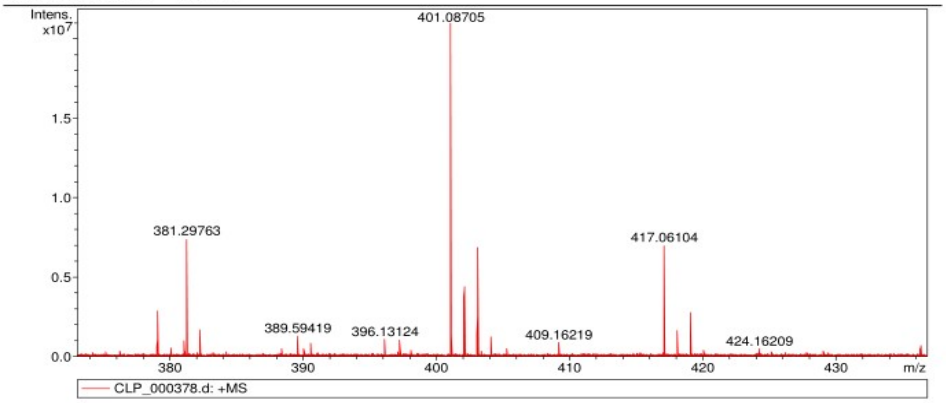

1

2 **Z2**

3

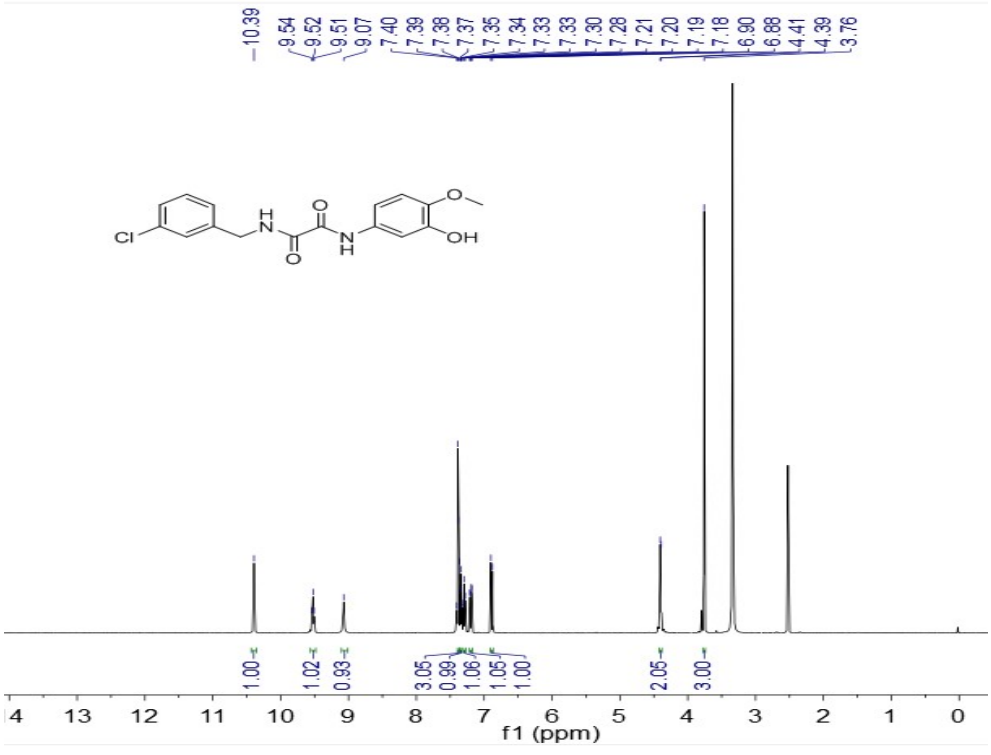

4

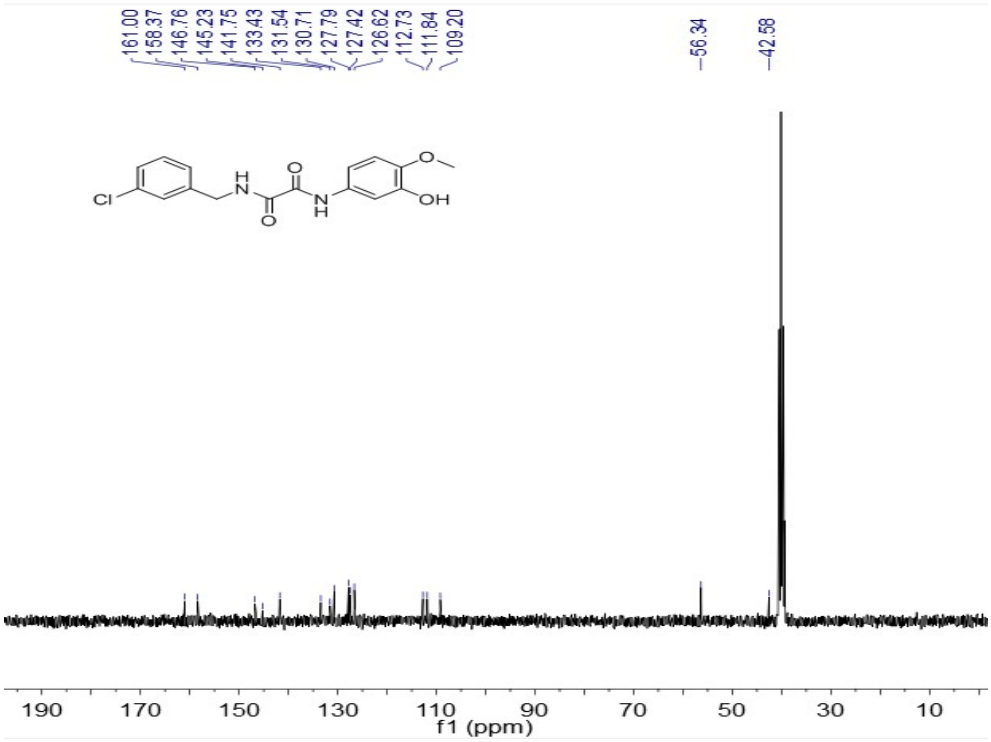

1

System Verification of Internal Mass Accuracy ESI Mode

Analysis Info

Analysis Name	D:\Data\HYY\CLP_000391.d	Acquisition Date	6/2/2021 2:35:26 PM
Method	4_19_MassAccuNeg	Operator	
Sample Name	58	Instrument	solariX
Comment	Glu-Fib 250amol		

Acquisition Parameter

Polarity	Positive	n/a	n/a	No. of Laser Shots	200
n/a	n/a	No. of Cell Fills	1	Laser Power	20.0 lp
Broadband Low Mass	53.8 m/z	n/a	n/a	n/a	n/a
Broadband High Mass	1000.0 m/z	n/a	n/a	n/a	n/a
Acquisition Mode	Single MS	n/a	n/a		
Pulse Program	basic	n/a	n/a	Calibration Date	Fri Feb 21 02:36:54 2014
Source Accumulation	0.020 sec	n/a	n/a	Data Acquisition Size	2097152
Ion Accumulation Time	0.200 sec	n/a	n/a	Apodization	Sine-Bell Multiplication
Flight Time to Acq. Cell	0.001 sec				

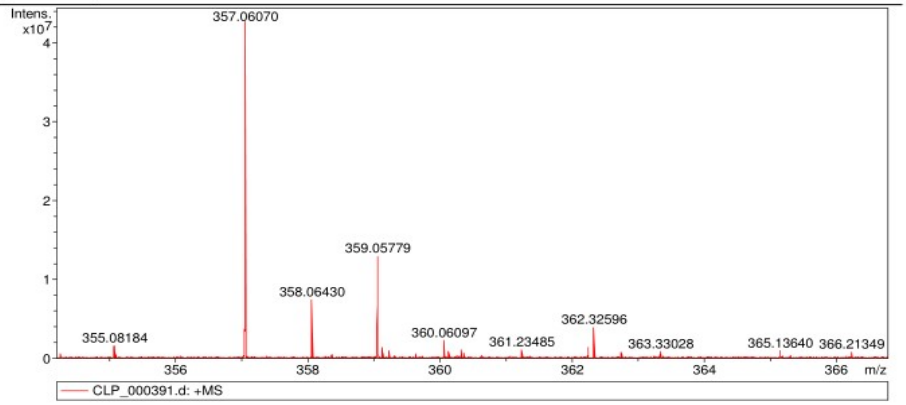

2

3 **Z3**

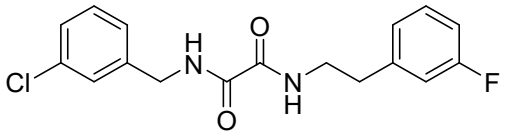

4

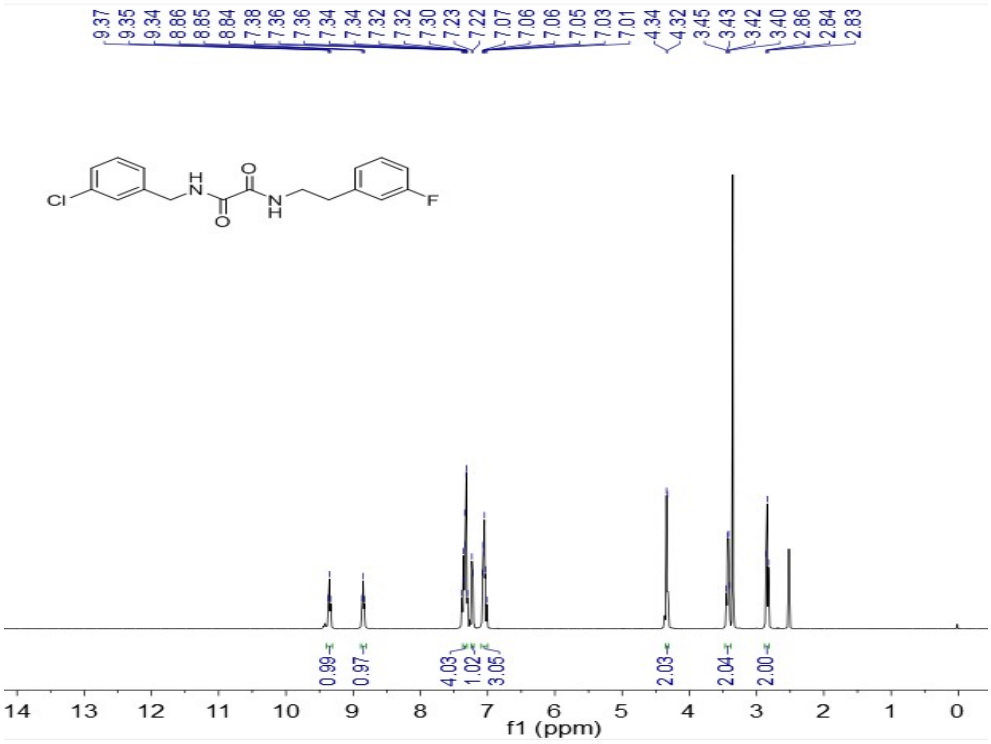
9.37
9.35
9.34
8.86
8.85
8.84
7.38
7.36
7.36
7.34
7.34
7.32
7.32
7.30
7.23
7.22
7.07
7.06
7.06
7.05
7.03
7.01
4.34
4.32
3.45
3.43
3.42
3.40
2.86
2.84
2.83
Cl
F
0.99
0.97
4.03
1.02
3.05
2.03
2.04
2.00
f1 (ppm)

1

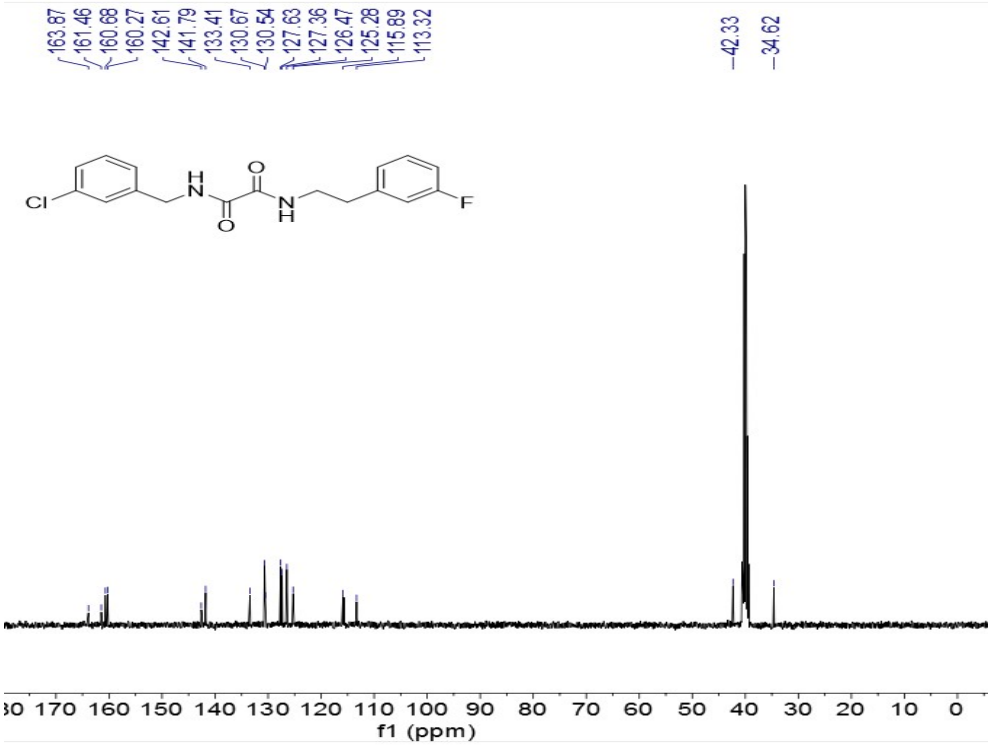
163.87
161.46
160.68
160.27
142.61
141.79
133.41
130.67
130.54
127.63
127.36
126.47
125.28
115.89
113.32
42.33
34.62
Cl
F
f1 (ppm)

2

System Verification of Internal Mass Accuracy ESI Mode

Analysis Info

Analysis Name	D:\Data\HYY\CLP_000379.d	Acquisition Date	6/2/2021 2:22:25 PM
Method	4_19_MassAccuNeg	Operator	
Sample Name	58	Instrument	solariX
Comment	Glu-Fib 250amol		

Acquisition Parameter

Polarity	Positive	n/a	n/a	No. of Laser Shots	200
n/a	n/a	No. of Cell Fills	1	Laser Power	20.0 lp
Broadband Low Mass	53.8 m/z	n/a	n/a	n/a	n/a
Broadband High Mass	1000.0 m/z	n/a	n/a	n/a	n/a
Acquisition Mode	Single MS	n/a	n/a		
Pulse Program	basic	n/a	n/a	Calibration Date	Fri Feb 21 02:36:54 2014
Source Accumulation	0.020 sec	n/a	n/a	Data Acquisition Size	1048576
Ion Accumulation Time	0.200 sec	n/a	n/a	Apodization	Sine-Bell Multiplication
Flight Time to Acq. Cell	0.001 sec				

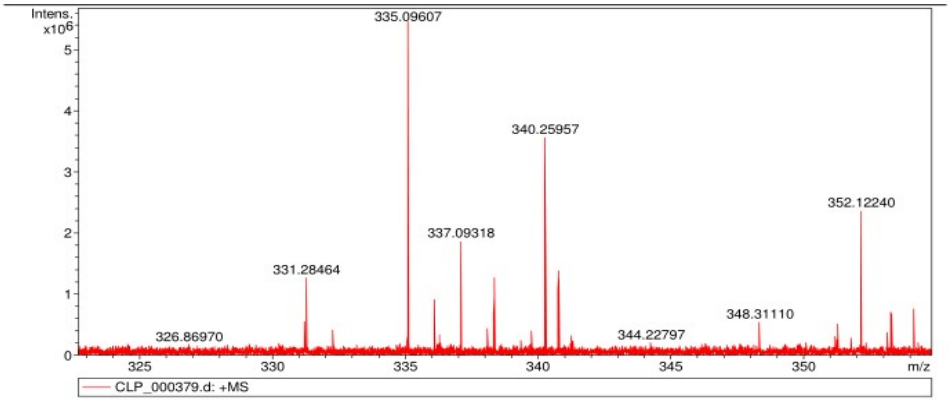

1

2 **Z4**

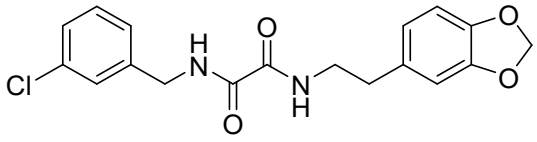

3

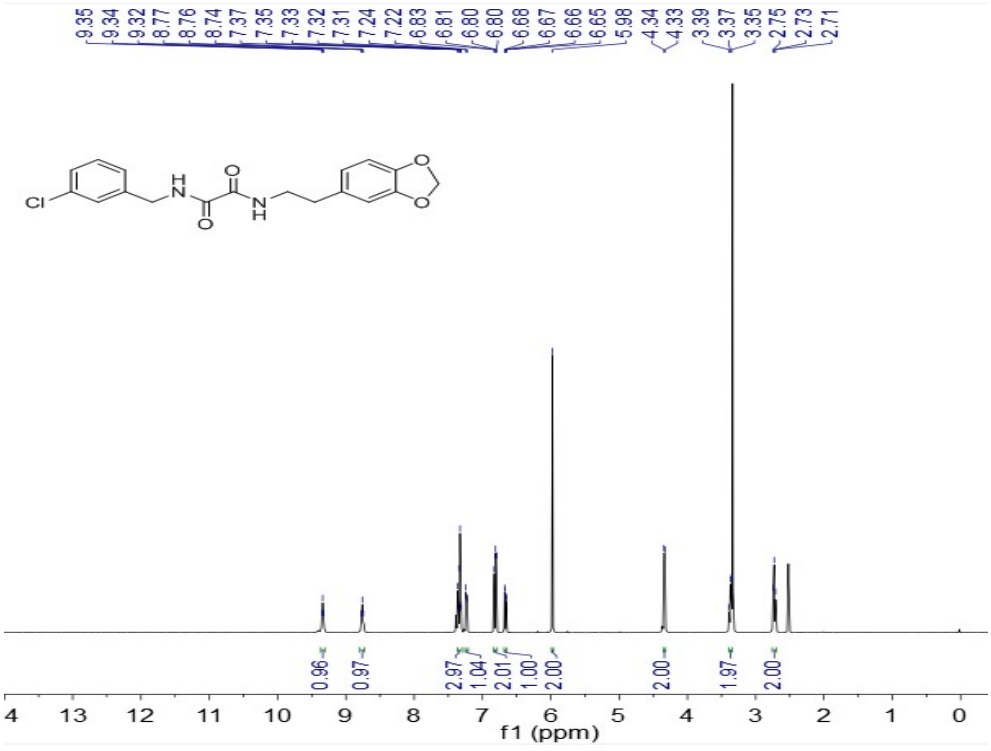

4

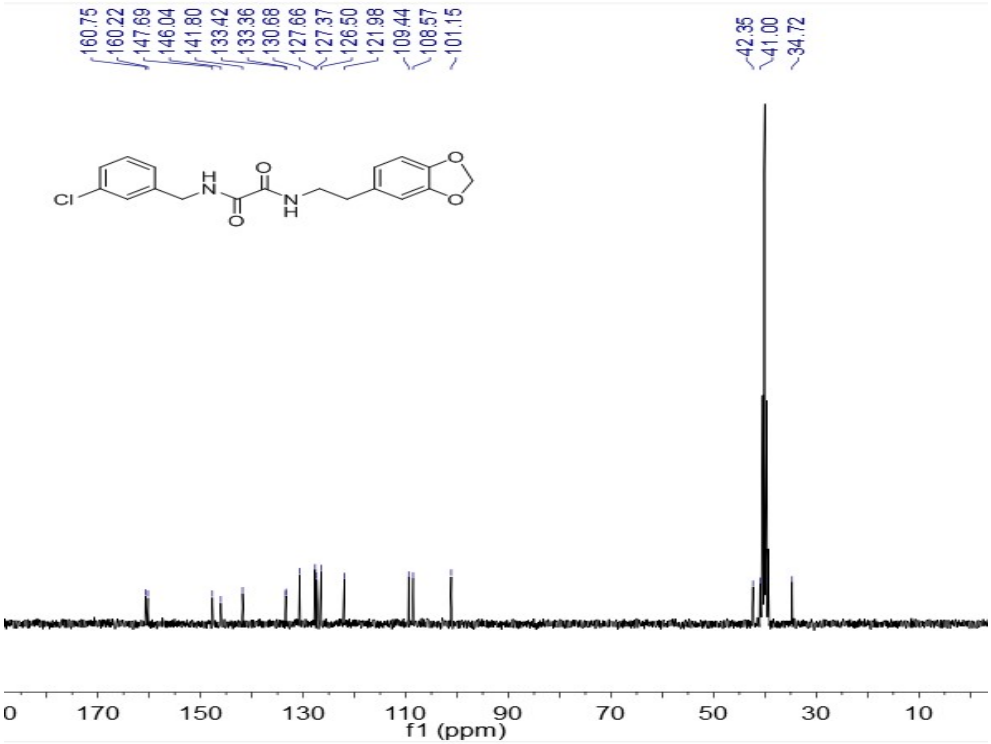
160.75
160.22
147.69
146.04
141.80
133.42
133.36
130.68
127.66
127.37
126.50
121.98
109.44
108.57
101.15
42.35
41.00
34.72
Cl
H
N
O
O
N
H
O
O
0
170
150
130
110
90
70
50
30
10
f1 (ppm)

1

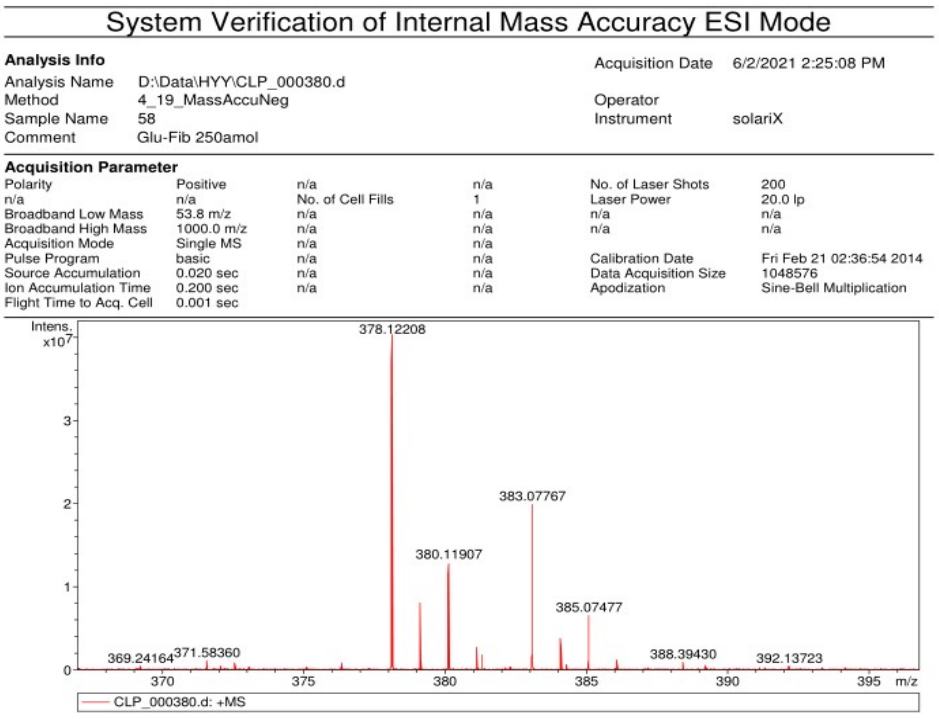
System Verification of Internal Mass Accuracy ESI Mode
Analysis Info
Analysis Name D:\Data\HYY\CLP_000380.d
Method 4_19_MassAccuNeg
Sample Name 58
Comment Glu-Fib 250amol
Acquisition Date 6/2/2021 2:25:08 PM
Operator
Instrument solariX
Acquisition Parameter
Polarity Positive
Broadband Low Mass 53.8 m/z
Broadband High Mass 1000.0 m/z
Acquisition Mode Single MS
Pulse Program basic
Source Accumulation 0.020 sec
Ion Accumulation Time 0.200 sec
Flight Time to Acq. Cell 0.001 sec
No. of Cell Fills 1
No. of Laser Shots 200
Laser Power 20.0 lp
Calibration Date Fri Feb 21 02:36:54 2014
Data Acquisition Size 1048576
Apodization Sine-Bell Multiplication
Intens.
x10^7
378.12208
383.07767
380.11907
385.07477
369.24164
371.58360
388.39430
392.13723
m/z
CLP_000380.d: +MS

2

3 **Z5**

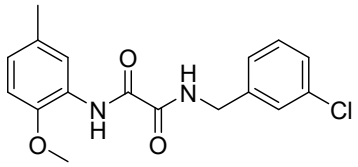
O
H
N
N
H
O
Cl
O

4

1

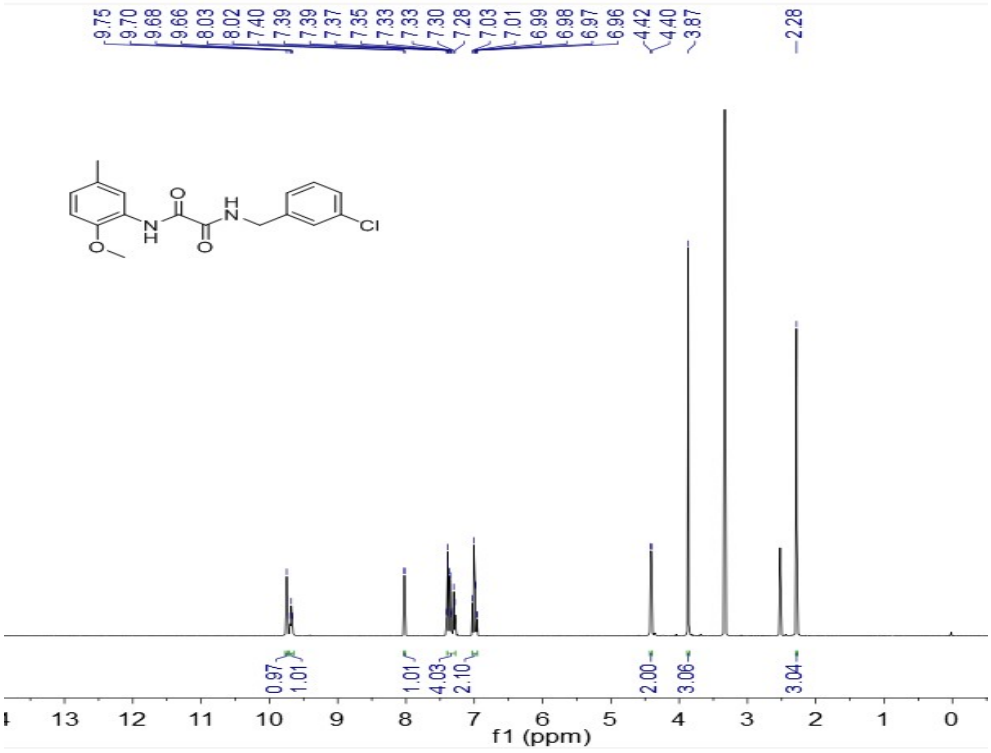
9.75
9.70
9.68
9.66
8.03
8.02
7.40
7.39
7.39
7.37
7.35
7.33
7.33
7.30
7.28
7.03
7.01
6.99
6.98
6.97
6.96
4.42
4.40
3.87
2.28
0.97
1.01
1.01
4.03
2.10
2.00
3.06
3.04
f1 (ppm)

2

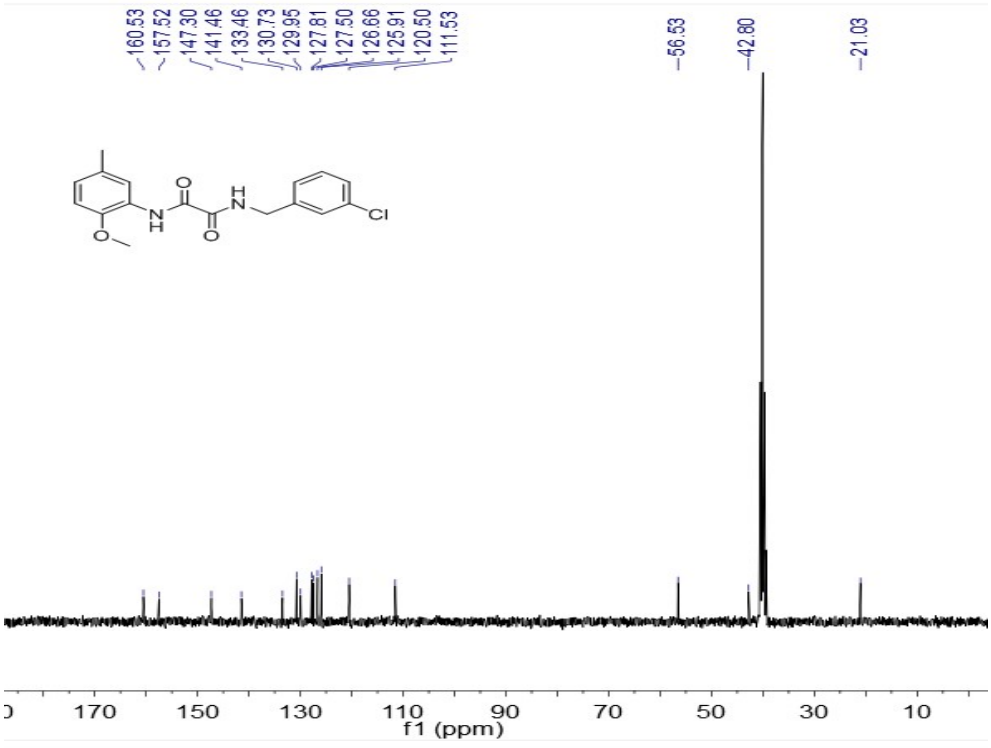
160.53
157.52
147.30
141.46
133.46
130.73
129.95
127.81
127.50
126.66
125.91
120.50
111.53
56.53
42.80
21.03
f1 (ppm)

System Verification of Internal Mass Accuracy ESI Mode

Analysis Info

Analysis Name	D:\Data\HYY\CLP_000384.d	Acquisition Date	6/2/2021 2:30:08 PM
Method	4_19_MassAccuNeg	Operator	
Sample Name	58	Instrument	solariX
Comment	Glu-Fib 250amol		

Acquisition Parameter

Polarity	Positive	n/a	n/a	No. of Laser Shots	200
n/a	n/a	No. of Cell Fills	1	Laser Power	20.0 lp
Broadband Low Mass	53.8 m/z	n/a	n/a	n/a	n/a
Broadband High Mass	1000.0 m/z	n/a	n/a	n/a	n/a
Acquisition Mode	Single MS	n/a	n/a		
Pulse Program	basic	n/a	n/a	Calibration Date	Fri Feb 21 02:36:54 2014
Source Accumulation	0.020 sec	n/a	n/a	Data Acquisition Size	1048576
Ion Accumulation Time	0.200 sec	n/a	n/a	Apodization	Sine-Bell Multiplication
Flight Time to Acq. Cell	0.001 sec				

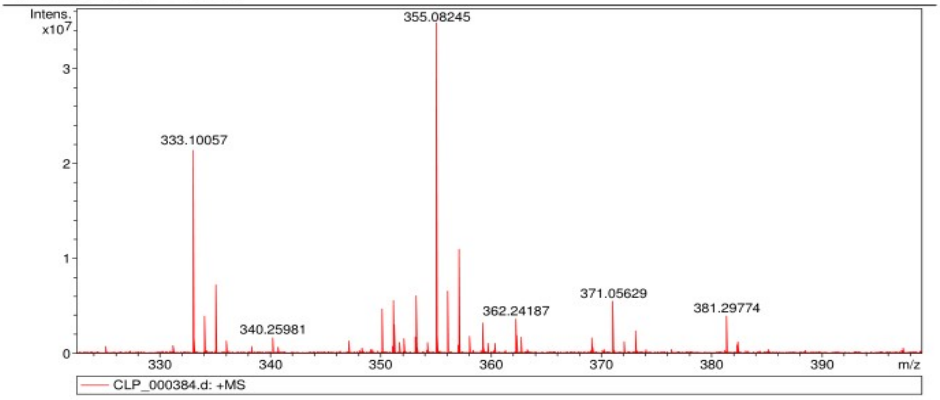

1

2 **Z6**

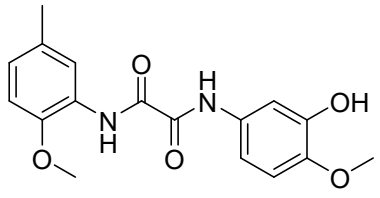

3

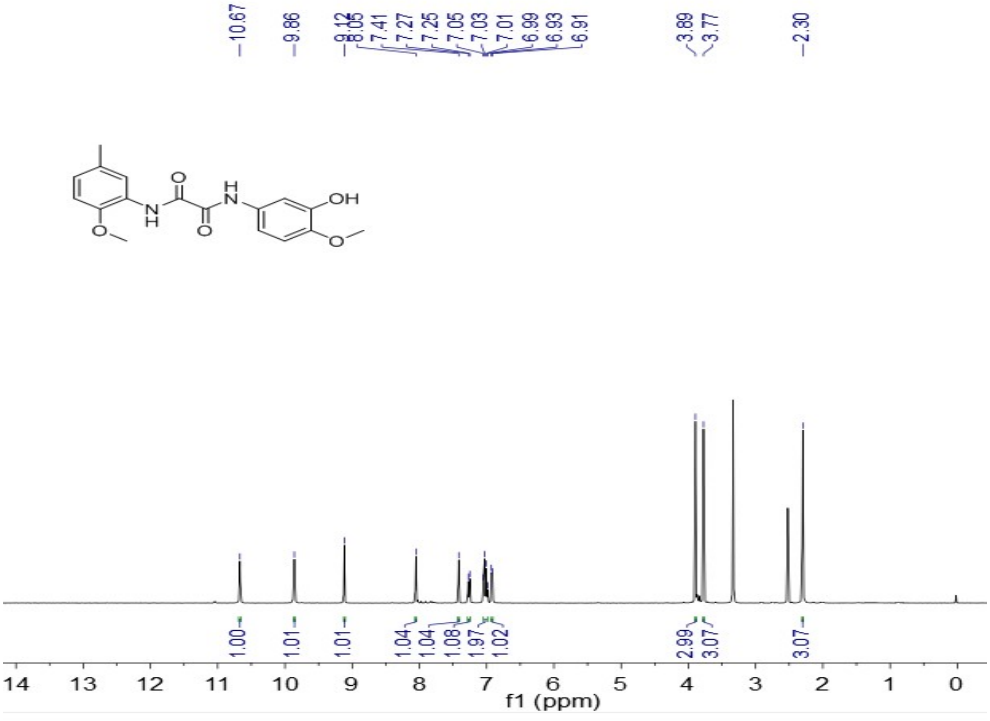

4

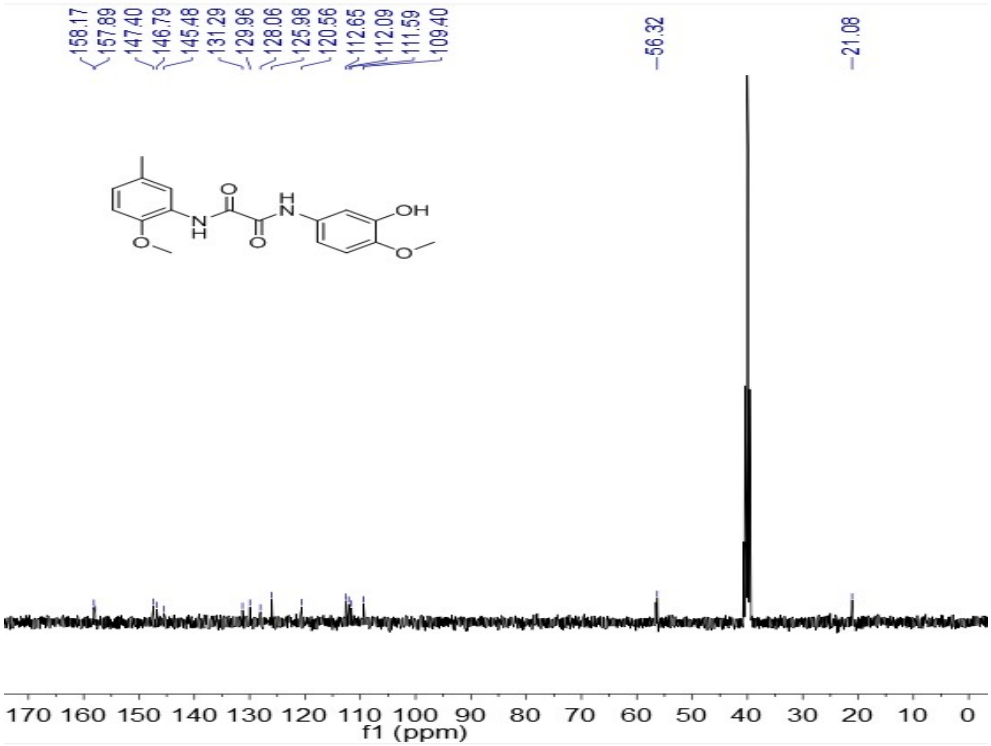

1

System Verification of Internal Mass Accuracy ESI Mode

Analysis Info

Analysis Name	D:\Data\HYY\CLP_000371.d	Acquisition Date	5/26/2021 9:37:48 AM
Method	4_19_MassAccuNeg	Operator	
Sample Name	58	Instrument	solariX
Comment	Glu-Fib 250amol		

Acquisition Parameter

Polarity	Positive	n/a	n/a	No. of Laser Shots	200
n/a	n/a	No. of Cell Fills	1	Laser Power	20.0 lp
Broadband Low Mass	53.8 m/z	n/a	n/a	n/a	n/a
Broadband High Mass	1000.0 m/z	n/a	n/a	n/a	n/a
Acquisition Mode	Single MS	n/a	n/a		
Pulse Program	basic	n/a	n/a	Calibration Date	Fri Feb 21 02:36:54 2014
Source Accumulation	0.020 sec	n/a	n/a	Data Acquisition Size	1048576
Ion Accumulation Time	0.200 sec	n/a	n/a	Apodization	Sine-Bell Multiplication
Flight Time to Acq. Cell	0.001 sec				

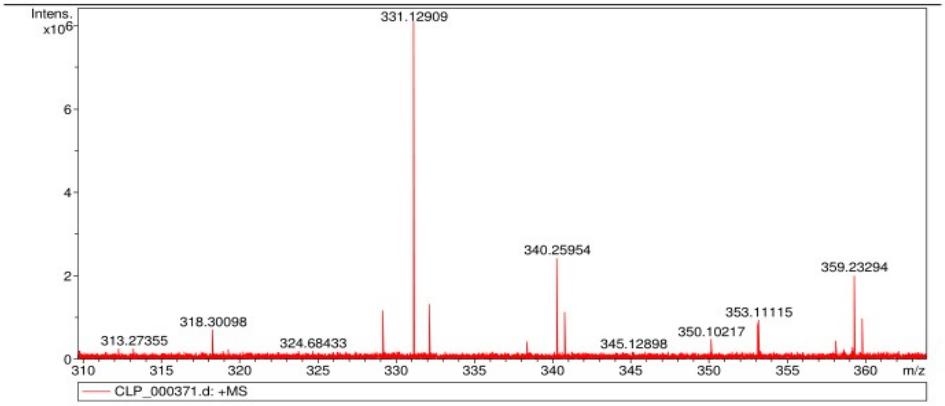

2

3 **Z7**

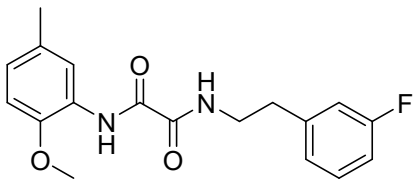

4

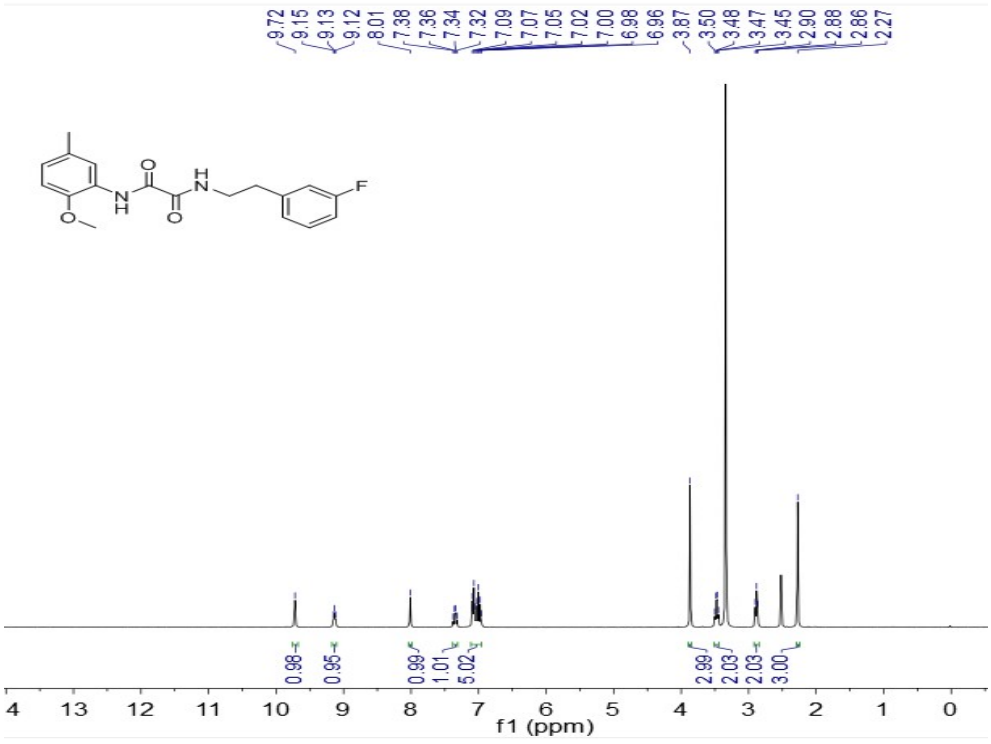
9.72
9.15
9.13
9.12
8.01
7.38
7.36
7.34
7.32
7.09
7.07
7.05
7.02
7.00
6.98
6.96
3.87
3.50
3.48
3.47
3.45
2.90
2.88
2.86
2.27
0.98
0.95
0.99
1.01
5.02
2.99
2.03
2.03
3.00
f1 (ppm)

1

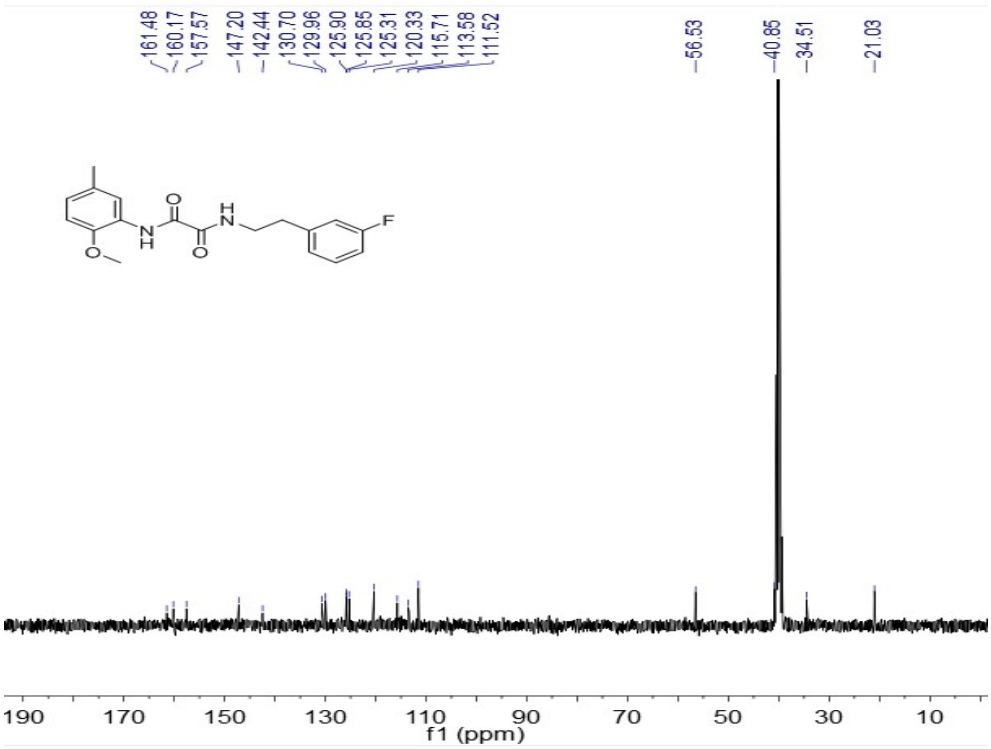
161.48
160.17
157.57
147.20
142.44
130.70
129.96
125.90
125.85
125.31
120.33
115.71
113.58
111.52
56.53
40.85
34.51
21.03
f1 (ppm)

2

System Verification of Internal Mass Accuracy ESI Mode

Analysis Info

Analysis Name	D:\Data\HYY\CLP_000395.d	Acquisition Date	6/2/2021 2:41:21 PM
Method	4_19_MassAccuNeg	Operator	
Sample Name	58	Instrument	solariX
Comment	Glu-Fib 250amol		

Acquisition Parameter

Polarity	Positive	n/a	n/a	No. of Laser Shots	200
n/a	n/a	No. of Cell Fills	1	Laser Power	20.0 lp
Broadband Low Mass	53.8 m/z	n/a	n/a	n/a	n/a
Broadband High Mass	1000.0 m/z	n/a	n/a	n/a	n/a
Acquisition Mode	Single MS	n/a	n/a		
Pulse Program	basic	n/a	n/a	Calibration Date	Fri Feb 21 02:36:54 2014
Source Accumulation	0.020 sec	n/a	n/a	Data Acquisition Size	1048576
Ion Accumulation Time	0.200 sec	n/a	n/a	Apodization	Sine-Bell Multiplication
Flight Time to Acq. Cell	0.001 sec				

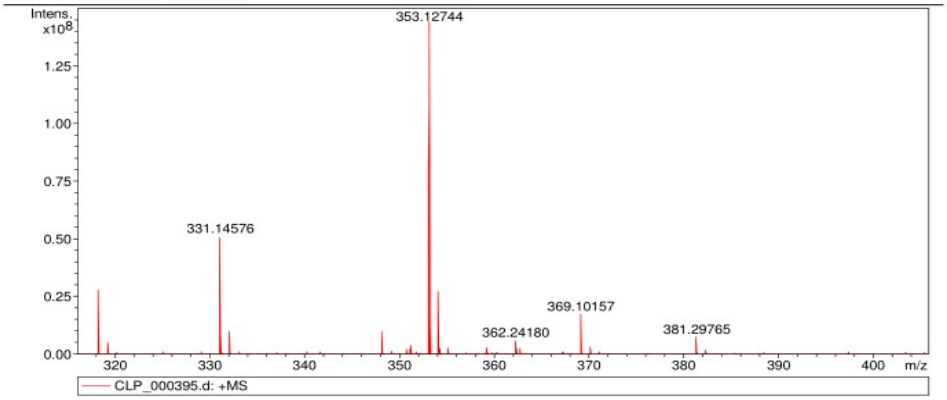

1

2 **Z8**

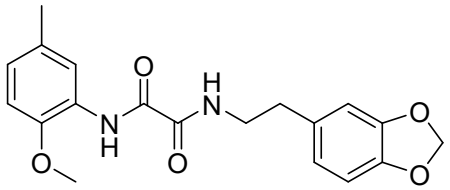

3

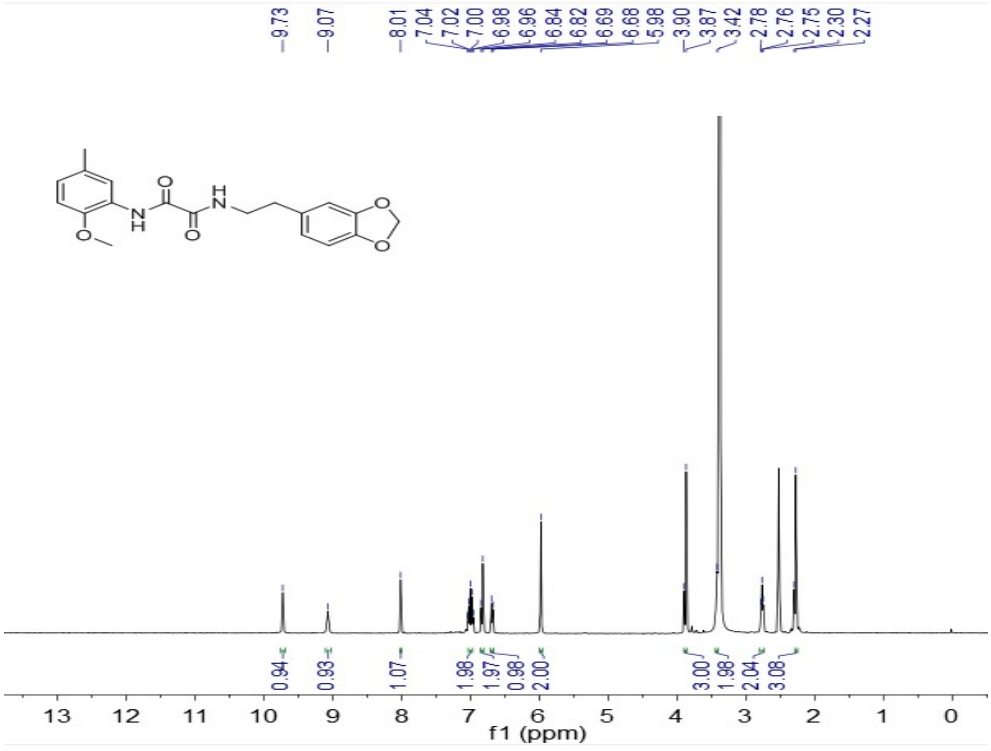

4

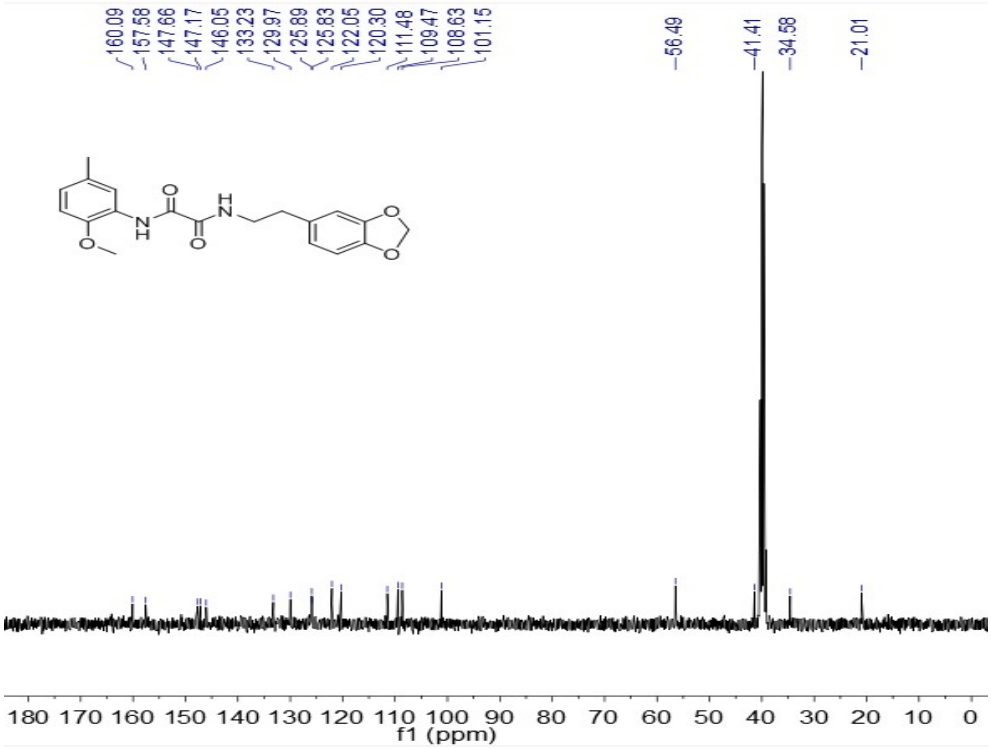

1

System Verification of Internal Mass Accuracy ESI Mode

Analysis Info

Analysis Name	D:\Data\HYY\CLP_000372.d	Acquisition Date	5/26/2021 9:40:36 AM
Method	4_19_MassAccuNeg	Operator	
Sample Name	58	Instrument	solariX
Comment	Glu-Fib 250amol		

Acquisition Parameter

Polarity	Positive	n/a	n/a	No. of Laser Shots	200
n/a	n/a	No. of Cell Fills	1	Laser Power	20.0 lp
Broadband Low Mass	53.8 m/z	n/a	n/a	n/a	n/a
Broadband High Mass	1000.0 m/z	n/a	n/a	n/a	n/a
Acquisition Mode	Single MS	n/a	n/a		
Pulse Program	basic	n/a	n/a	Calibration Date	Fri Feb 21 02:36:54 2014
Source Accumulation	0.020 sec	n/a	n/a	Data Acquisition Size	1048576
Ion Accumulation Time	0.200 sec	n/a	n/a	Apodization	Sine-Bell Multiplication
Flight Time to Acq. Cell	0.001 sec				

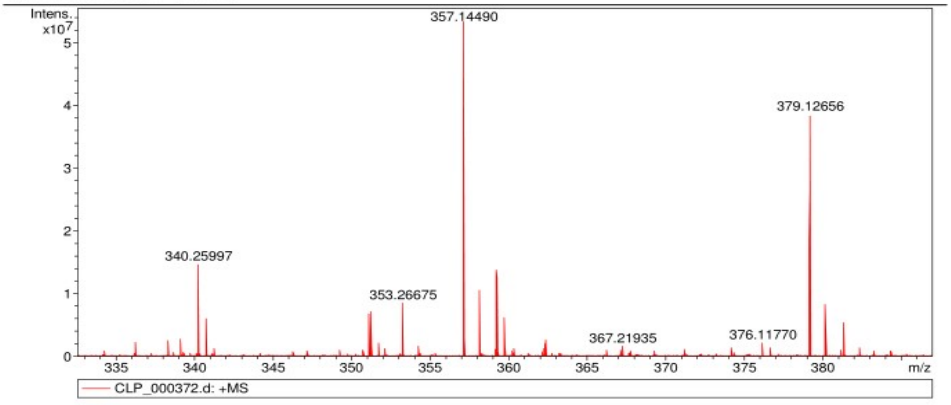

2

3 **Z9**

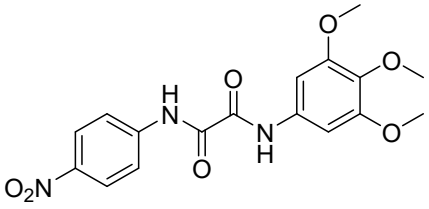

4

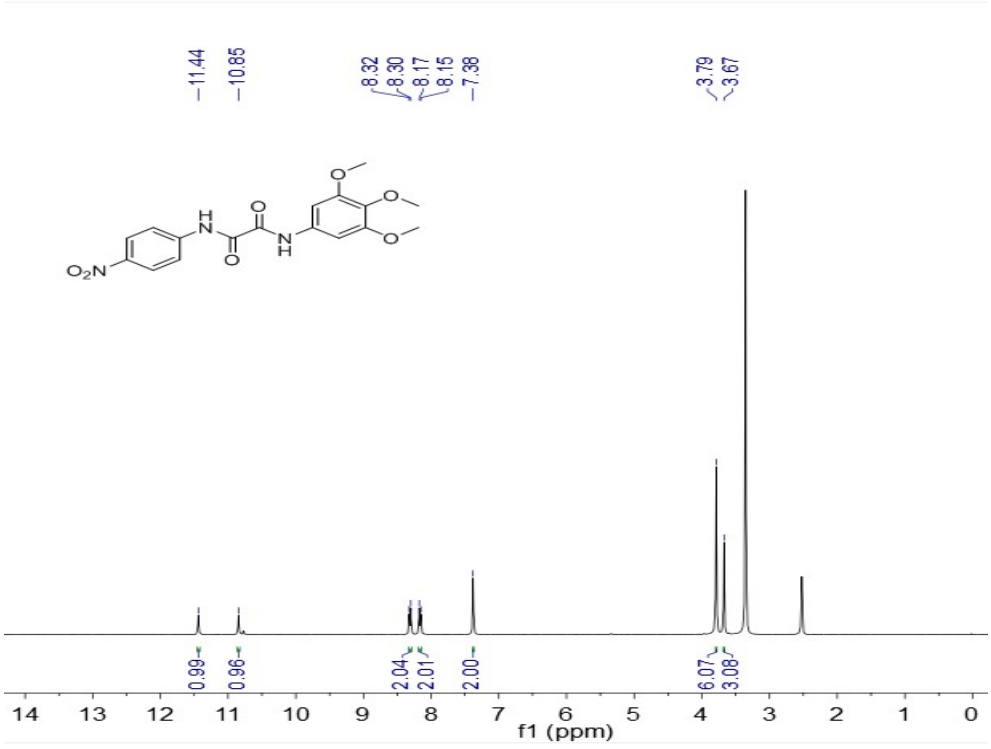
11.44
10.85
8.32
8.30
8.17
8.15
7.38
3.79
3.67
0.99
0.96
2.04
2.01
2.00
6.07
3.08
f1 (ppm)

1

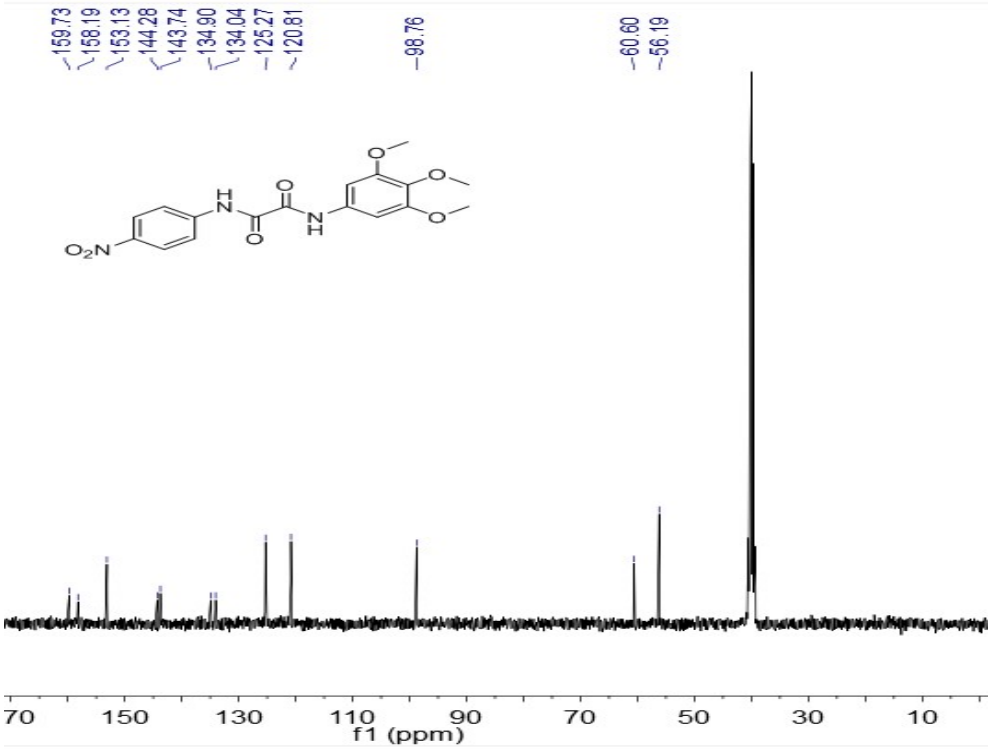
159.73
158.19
153.13
144.28
143.74
134.90
134.04
125.27
120.81
98.76
60.60
56.19
f1 (ppm)

2

System Verification of Internal Mass Accuracy ESI Mode

Analysis Info

Analysis Name	D:\Data\HYY\CLP_000369.d	Acquisition Date	5/26/2021 9:30:30 AM
Method	4_19_MassAccuNeg	Operator	
Sample Name	58	Instrument	solariX
Comment	Glu-Fib 250amol		

Acquisition Parameter

Polarity	Positive	n/a	n/a	No. of Laser Shots	200
n/a	n/a	No. of Cell Fills	1	Laser Power	20.0 lp
Broadband Low Mass	53.8 m/z	n/a	n/a	n/a	n/a
Broadband High Mass	1000.0 m/z	n/a	n/a	n/a	n/a
Acquisition Mode	Single MS	n/a	n/a		
Pulse Program	basic	n/a	n/a	Calibration Date	Fri Feb 21 02:36:54 2014
Source Accumulation	0.020 sec	n/a	n/a	Data Acquisition Size	1048576
Ion Accumulation Time	0.200 sec	n/a	n/a	Apodization	Sine-Bell Multiplication
Flight Time to Acq. Cell	0.001 sec				

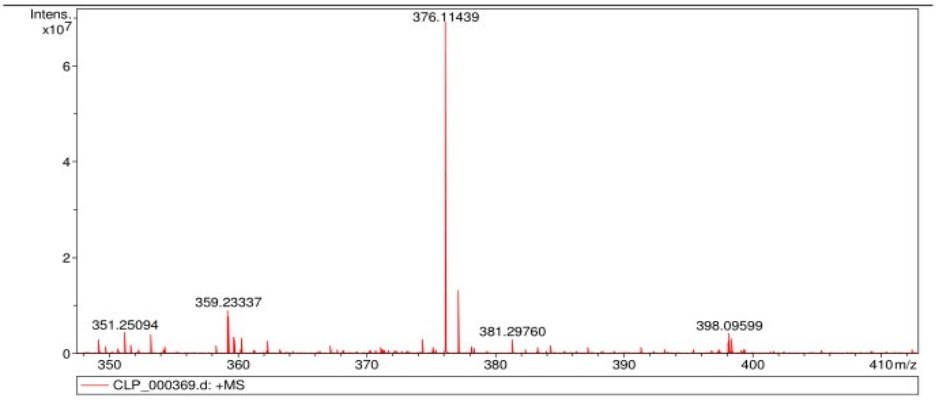

1

2 **Z10**

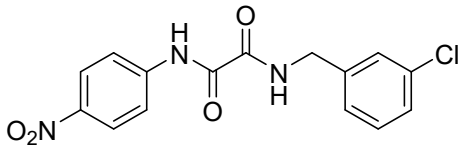

3

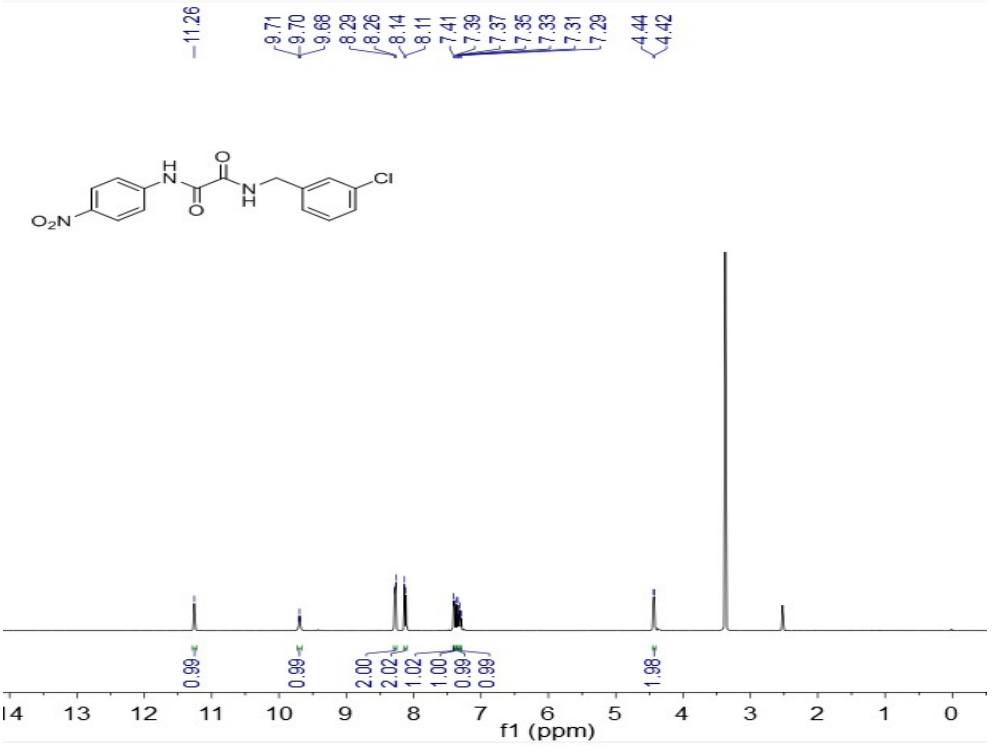

4

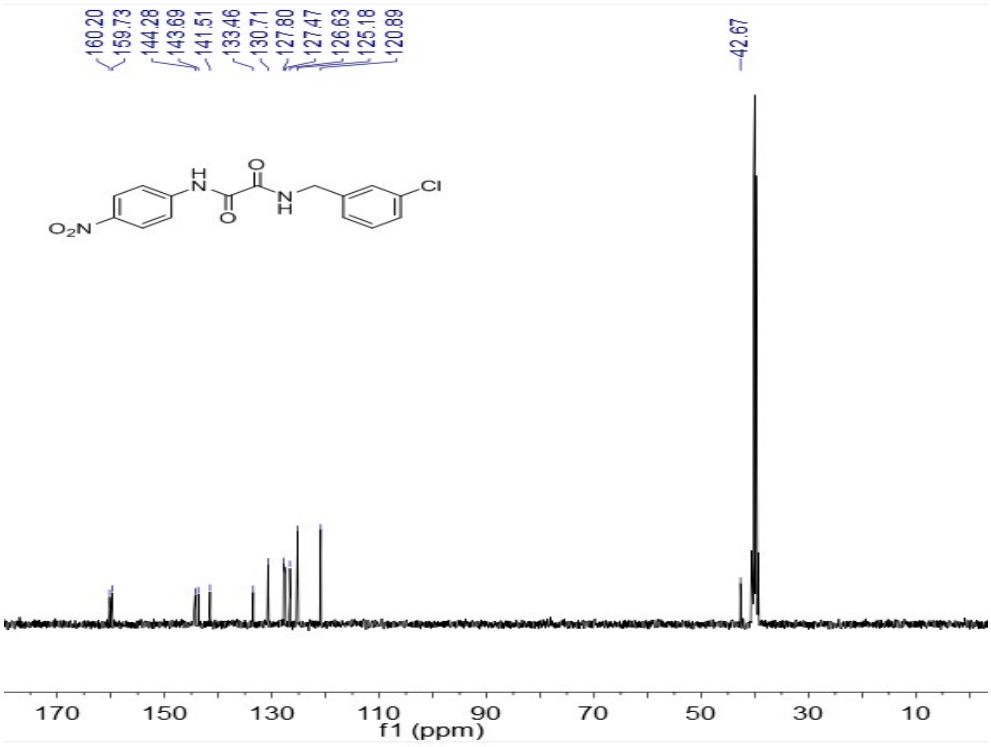

1

System Verification of Internal Mass Accuracy ESI Mode

Analysis Info

Analysis Name	D:\Data\HYY\CLP_000377.d	Acquisition Date	6/2/2021 2:14:27 PM
Method	4_19_MassAccuNeg	Operator	
Sample Name	58	Instrument	solariX
Comment	Glu-Fib 250amol		

Acquisition Parameter

Polarity	Positive	n/a	n/a	No. of Laser Shots	200
n/a	n/a	No. of Cell Fills	1	Laser Power	20.0 lp
Broadband Low Mass	53.8 m/z	n/a	n/a	n/a	n/a
Broadband High Mass	1000.0 m/z	n/a	n/a	n/a	n/a
Acquisition Mode	Single MS	n/a	n/a		
Pulse Program	basic	n/a	n/a	Calibration Date	Fri Feb 21 02:36:54 2014
Source Accumulation	0.020 sec	n/a	n/a	Data Acquisition Size	1048576
Ion Accumulation Time	0.200 sec	n/a	n/a	Apodization	Sine-Bell Multiplication
Flight Time to Acq. Cell	0.001 sec				

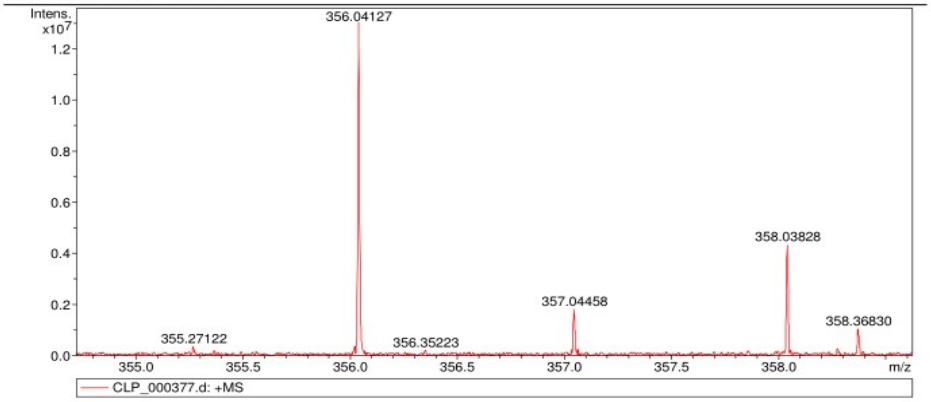

2

3

4 5. Biological assays

5 5.1 Neuraminidase inhibition assay

6 The neuraminidase (H5N1 and H5N1-H274Y) was purchased from Sino Biological

Inc. (China). 2-N-mopholino-ethanesulfonic acid (MES) and 4-methylumbelliferyl-α-D-N-acetylneuraminicacidsodium salt hydrate (4-MUNANA) were purchased from Sigma. 4-methylumbelliferone (4-MU) was purchased from Shanghai Standard Technology Co., Ltd. The enzyme assay was performed by using the previously reported method with slight modifications.[13] The tested compounds were dissolved in DMSO firstly and then diluted into 6 concentration gradients. For each tested compound **5** and **Z1-Z10**, a set of solutions with concentrations span the range 0.064 μM to 200 μM. In general, 10 μL of NA, 70 μL buffer solution (33 mM MES, 4 mM $CaCl_2$), and 10 μL of different concentrations of samples were added to each well of the 96-well plate. Then the 96-well plate was placed and shocked for 1 minute in the multifunctional fluorescent enzyme-labeled instrument and the temperature was set at 37℃, so that the NA enzyme and the sample to be tested could be fully mixed. The mixture was incubated at 37℃ for 15 minutes. 10 μL of 100 μM fluorescent substrate (4-MUNANA) solution was also added to each well. Next, the plate was placed in the multifunctional fluorescent enzyme-labeled instrument again. It was shaken for 1 minute and then incubated at 37℃ for 60 minutes. The reaction was terminated by adding 150 μL of stop solution (14 $mmol \cdot L^{-1}$ NaOH containing 83% ethanol). Finally, the resulting fluorescence was measured at an excitation wavelength of 355 nm and an emission wavelength of 460 nm, respectively. Parallel experiments were performed three times. The oseltamivir acid was used as a positive control in the enzyme inhibition assay. The inhibition curves were drawn by GraphPad Prism 5.0 software and the IC_{50} values were calculated by using enzyme inhibition rate and concentration data. The IC_{50} (μM) is presented as mean ± SD from at least three independent tests.

5.2 In vitro anti-influenza virus assay and cytotoxicity assay

The *in vitro* anti-influenza virus assay and cytotoxicity assay for compound **Z2** were performed according to the previously described methodology with slight modifications.[14] The anti-influenza virus activity of compound **Z2** was assessed in Madin-Darby canine kidney (MDCK) cells by CCK-8 method. The CPE of influenza virus infection using A/chicken/Hubei/327/2004 (H5N1-DW) as representative of group-1 NAs-containing influenza strain. The results of EC_{50} values were described the concentrations affording 50% protection against H5N1 virus infection-mediated CPE. Aliquots of 50 μL of diluted H5N1 were mixed with equal volumes of solutions of the compound **Z2** in serial 2-fold dilutions in assay media (DMEM). The mixtures were used to infect 100 μL of CEF at $1x10^5$ cells/mL in 96-well plates. At 37℃ under 5.0% CO_2 in air, the plates were incubated for 48 h. Then, to each well, 10 μL kit-8

(CCK-8) reagent solution and 100 μL media was added. After incubation at 37 °C for 90 min, the absorbance at 450 nm was read on a microplate reader. Inhibitor EC_{50} values were determined by fitting the curve of percent CPE versus inhibitor concentration. OSC was used as a control drugs at the same time. The CC_{50} value was used to measure the cytotoxicity of the test compounds to MDCK cells and was determined in the same manner as EC_{50} but without virus infection.

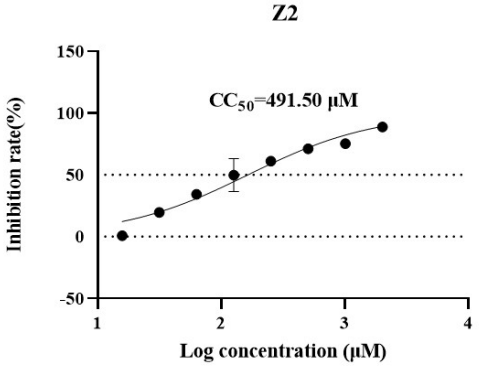

Fig. S3 The CC_{50} profile of the most potent NA inhibitor **Z2**

References

1. Lengauer T, Rarey M. Computational methods for biomolecular docking, *Curr. Opin. Struc. Biol.* 1996; 6: 402-406.

2. Gschwend D A, Good A C, Kuntz I D. Molecular docking towards drug discovery, *J. Mol. Recognit.* 1996; 9: 175-186.

3. Russell R J, Haire L F, Stevens D J, et al. The structure of H5N1 avian influenza neuraminidase suggests new opportunities for drug design, *Nature.* 2006; 443: 45-49.

4. Jain A N. Surflex: fully automatic flexible molecular docking using a molecular similarity-based search engine, *J. Med. Chem.* 2003; 46: 499-511.

5. Vay J L, Fawley W. AMBER User's Manual, 2000.

6. Hornak V, Abel R, Okur A, et al. Comparison of multiple Amber force fields and development of improved protein backbone parameters, *Proteins.* 2006; 65: 712-725.

7. Wang J, Wolf R M, Caldwell J W, et al. Development and testing of a general amber force field, *J. Comput. Chem.* 2004; 25: 1157-1174.

8. Sun H, Li Y, Shen M, et al. Assessing the performance of MM/PBSA and MM/GBSA methods. 5. Improved docking performance using high solute dielectric constant MM/GBSA and MM/PBSA rescoring, *Phys. Chem. Chem. Phys.* 2014; 16: 22035-22045.

9. Darden T, York D, Pedersen L. Particle mesh Ewald: An N· log (N) method for Ewald sums in large systems, *J. Chem. Phys.* 1993; 98: 10089-10092.
10. Hou T, Wang J, Li Y, et al. Assessing the performance of the MM/PBSA and MM/GBSA methods. 1. The accuracy of binding free energy calculations based on molecular dynamics simulations, *J. Chem. Inf. Model.* 2011; 51: 69-82.
11. Liu M, Yuan M, Luo M, et al. Binding of curcumin with glyoxalase I: Molecular docking, molecular dynamics simulations, and kinetics analysis, *Biophys. Chem.* 2010; 147: 28-34.
12. Massova I, Kollman P A. Combined molecular mechanical and continuum solvent approach (MM-PBSA/GBSA) to predict ligand binding, *Perspect. Drug. Discov.* 2000; 18: 113-135.
13. Wang K, Yang F, Wang L, et al. Synthesis and biological evaluation of NH2-acyl oseltamivir analogues as potent neuraminidase inhibitors, *Eur. J. Med. Chem.* 2017; 141: 648-656.
14. Zhang J, Murugan N A, Tian Y, et al. Structure-based optimization of N-substituted oseltamivir derivatives as potent anti-Influenza A virus agents with significantly improved potency against oseltamivir-resistant N1-H274Y variant, *J. Med. Chem.* 2018; 61: 9976-9999.